UNIVERSITÀ
DEGLI STUDI
DI PADOVA

UNIVERSITÀ DEGLI STUDI DI PADOVA

ENGINEERING INDUSTRIAL DEPARTMENT

MASTER DEGREE IN CHEMICHAL AND INDUSTRIAL PROCESS ENGINEERING

Master thesis in
Chemical and Industrial Process Engineering

THERMAL AND KINETIC STUDY OF SOYBEAN OIL EPOXIDATION IN A CALORIMETRIC REACTOR

Supervisor: Prof. Giuseppe Maschio

Co-supervisor: Ph.D. Paolo Mocellin

Dott. Damiano Piccolo

Candidate: ANDREA ROSSI

ACADEMIC YEAR 2017-2018

Riassunto

Nel presente elaborato viene descritto il lavoro svolto durante l'attività di tirocinio perfezionata presso l'Università degli Studi di Padova. Lo scopo di tale lavoro è consistito nell'esecuzione di uno studio termico e cinetico sulla reazione di epossidazione di olio di soia utilizzando acido peracetico in un reattore calorimetrico.

L'olio di soia epossidato (comunemente chiamato ESBO) viene largamente utilizzato come plastificante e stabilizzante nel PVC. Inoltre, in seguito al divieto di impiego di diversi ftalati dovuto al loro nocività sulla salute umana, l'olio di soia epossidato rappresenta una possibile alternativa non tossica e sostenibile. L'olio di soia epossidato può essere inoltre utilizzato per produrre svariati intermedi tra i quali polioli per la sintesi di poliuretani e poliesteri.

Lo scopo principale di questo lavoro consiste nello studio del processo di epossidazione dell'olio di soia utilizzando acido perossicarbossilico ed acqua ossigenata in presenza di un catalizzatore acido liquido al fine di sviluppare un modello matematico descrittivo del processo in esame. Tale modello è stato sviluppato mediante software *MATLAB*®. Esso ha permesso di estrarre e dedurre informazioni riguardanti la cinetica delle reazioni coinvolte ed il trasferimento di massa tra le due fasi interessate nel processo.

Ciò a supporto di una migliore comprensione dei principali step limitanti associati al processo di epossidazione e degli aspetti rilevanti ai fini di scale-up del sistema di reazione.

Nel Capitolo 1 è contenuta una descrizione generale riguardante i diversi tipi di processo impiegati per l'epossidazione di oli vegetali. Verrà data attenzione al processo di epossidazione bifasica che è stato utilizzato nella parte sperimentale del presente lavoro. Nel Capitolo 2 viene invece illustrato il funzionamento del reattore nel quale è stata condotta la reazione di epossidazione, delle apparecchiature ausiliarie necessarie per il suo funzionamento e di quelle utilizzate per la realizzazione dello studio termico. Nel Capitolo 3 verrà spiegata nel dettaglio la procedura sperimentale necessaria per la raccolta dei dati sulla cui base è stato validato il modello matematico. L'approccio modellistico verrà infine illustrato nel Capitolo 4 con l'illustrazione dei risultati ottenuti dal modello stesso.

Abstract

The aim of this work focuses on a kinetic and thermal study of the soybean oil epoxidation reaction using peroxyacetic acid in a calorimetric reactor.

It is to remind that epoxidated soybean oil (commonly called ESBO) is largely used as plasticizer and stabilizer in PVC and, after the interdiction of many phthalates for their impact on human health, it represents an optimal sustainable nontoxic alternative. Epoxidized soybean oil can be also an intermediate for other products as polyols for the synthesis of polyurethane and polyesters.

The main objective is the study of the epoxidation of soybean oil using peroxycarboxylic acid and hydrogen peroxide in presence of an acid liquid catalyst in order to develop a mathematical model able to simulate this specific epoxidation process. The model is developed with *MATLAB*® and information regarding the contribute of the reaction kinetics and the mass transfer between the two phases involved is obtained. This allows for a better understanding of main rate limiting steps and topical aspects to be improved in an industrialization perspective. In addition, the heat exchange coefficient of the calorimetric reactor is determined.

Index

Introduction

This work involves the kinetic of epoxidation reaction of soybean oil using peroxycarboxylic acid in a calorimetric batch reactor in presence of a liquid acid as catalyst. In detail, this reaction is carried out using peroxyacetic acid as oxygen carrier, hydrogen peroxide as oxidant and sulphuric acid as catalyst. Both kinetic and mass transfer between aqueous and oleos phases are taken into account to establish which is the rate determining step of the process. The analysis is used also to support the model development.

The unsaturation of the vegetable oils rich in oleic, linoleic and linolenic acyl groups may be used to introduce functional groups like epoxides. The industrial production of epoxidized oils is carried out since 1946 with the first patent application [1].

Nowadays epoxidized oils are important chemicals which can be used in various domains, for example as stabilisers and plasticisers in polymers, as additive in lubricants, as component in plastics and urethane foams. More in general, epoxidized oils allow the production of many commodities totally bio-based preventing the use of petroleum-derived compounds. Epoxidized soybean oil is largely used as a co-stabilizer and a secondary plasticizer of PVC with a worldwide production of more than 2000 $\mathrm{kton/yr}$ [1]. The application of this material as a primary plasticizer of PVC and building block for other bio-based chemicals has been growing significantly due to better quality of the epoxidized products and improved competitiveness over petroleum based traditional materials. Furthermore, it represents an optimal substitute of phthalates as a plasticizer since phthalates have been banned in many countries for their negative effects on health. [2]

In the literature, several techniques are reported to perform oil epoxidation.

Epoxidation of vegetable oils can be carried out in solution or in bulk, with *in situ* or preformed peroxides. The most widely used process is the epoxidation of unsaturated compounds with peroxyacids formed *in situ* because when the peroxyacid is preformed, there are some safety issues as the concentrated peroxyacid is unstable and explosive [29].

The most commonly used technique is the biphasic epoxidation which requires oil, carboxylic acid, hydrogen peroxide and a liquid acid catalyst [2]. The reaction is carried out by reacting the double bonds of the oil with a peroxyacid (generally peroxyacetic or peroxyformic) generated in situ by reacting hydrogen peroxide with acetic or formic acid in the presence of a mineral acid as a catalyst (sulphuric, nitric or phosphoric acid). Two distinct phases are present: in the aqueous one the formation of the peroxyacid occurs which migrates into the oil phase and reacts with the double bonds of the fatty acid chains giving epoxide groups and regenerating the carboxylic acid. The regenerated acid moves back to the aqueous phase.

In the triphasic epoxidation oil, carboxylic acid, hydrogen peroxide and a solid catalyst are employed [3]. The mechanism is similar but, a solid catalyst like an acidic ion exchange resin

is used instead of a liquid one. The selectivity is improved with respect to the biphasic process once an appropriate solid catalyst is selected [4].

The multiphase epoxidation uses electrochemical technique. The involved substances are oil, formic and hydrochloric acid and gaseous O_2, [5]. In the cathodic compartment of the reactor H_2O_2 is produced, that oxidize formic acid which epoxidizes the oil. In the anodic compartment the oil is epoxidized reacting with chloridrine. The main advantages of this technique are the in-situ production of hydrogen peroxyde and the reduced time required for the reaction.

The term enhanced epoxidation includes all techniques similar to the biphasic and triphasic but performed via non-conventional heating technique such as microwaves and ultrasounds to improve the process efficiency.

As mentioned before, in the present work is carried out a biphasic epoxidation using soybean oil, hydrogen peroxide, acetic acid as oxygen carrier and sulphuric acid as catalyst.

As concerns this work, it is made of four chapters. Chapter 1 deals with a bibliographic review of the main method used to achieve epoxidation of vegetable oils with a particular focus on the optimal operating conditions to perform a bi-phasic epoxidation. Chapter 2 is focused on the description of the experimental apparatus utilized to carry out the experiments and how the stirring system of the reactor has been calibrated. Chapter 3 deals with materials and the experimental procedures followed to carry out both the epoxidation process and the thermal study of the system. In addition, the results of the thermal study are reported. Chapter 4 exposes the employed modeling approach and all the model results.

Chapter 1
Epoxidation of vegetable oils

Vegetable oils area valuable raw material extracted from biomass, in particular from plants, fruit seeds or wood. The global production of vegetable oils has been constantly increasing for the past decade, as its consumption. Approximately 80% of the total production of oils is employed in food industry, the rest is directed to the other purposes such as chemical industry and production of biofuels. Globally, the most used vegetable to produce oils is palm, followed by soybean and rapeseed. The world-wide consumption of these oils is, respectively, 60, 54 and 29 million metric tons in the years 2016/2017. In addition, the consumption forecast is going to increase [6].

Thanks to the epoxidation, from these oils polyols, glycols, olefinic compounds and stabilizers for polymers as well as plasticizers for developing PVC-derived plastic commodities can be produced. They are also very good biodegradable lubricants. In 2017 the global lubricants demand consisted in 35.7 million metric tons, mostly petroleum-based. Looking at the demand trend in the years it can be noticed that it has been increased from 2009 to date. The development of biolubricants from vegetable oils offers an eco-friendly and sustainable alternative to mineral oil-based lubricants. In addition, the cost of bio-based lubricants is higher than oil-based ones, but compared to maintenance and energy costs, it is a minor factor [26]. In fact, the latter route of production follows the philosophy of Green Chemistry, because there is no production of waste such as glycerol or the use of explosive reactants such as hydrogen [14].

1.1 Reaction of epoxidation: features and feasible techniques

The epoxidation consists in the formation of an epoxy group from the instaurations present in olefinic type of molecules, such as vegetable oils. This reaction consists in a partial oxidation of the fatty acid in which an atom of oxygen is introduced in the fatty acid chains where an instauration is present. A parallel reaction that involves the epoxy ring opening and produces α-glycol also occurs. The commercial value of an epoxidated product is higher if with a smaller percentage of α-glycol. To establish the quality of an epoxidated product it is useful to define quality parameters which are useful to indicate how much oil has been epoxidized and how much oil has been converted into by-products. It appears evident how these parameters reflect their importance on the economic value of the product. The quality parameters are defined below.

The double bond conversion is defined as:

$$C = C_{conversion} = \frac{[C{=}C]_{start} - [C{=}C]_{end}}{[C{=}C]_{end}} \cdot 100\%. \quad (1.1)$$

In Equation (1.1) $C = C$ stands for double bonds and square brackets indicates concentration, volumetric or massive (moles of double bonds per unit of mass or of volume of oil). The concentration of double bonds is assessed with the iodine number. This parameter indicates how many double bonds have reacted, but it doesn't tell anything about how many epoxy-rings have been formed. This information can be obtained from the relative percentage conversion to oxirane:

$$Relative\ conversion\ to\ oxirane = \frac{\%OO_{exp}}{\%OO_{the}} \cdot 100\%. \quad (1.2)$$

In Equation (1.2) $\%OO_{exp}$ indicates the content of oxirane oxygen experimentally found. It can be determined by direct method using hydrobromic acid solution in glacial acetic acid (Paquot, 1979). $\%OO_{the}$ is the maximum oxirane oxygen that can be theoretically determined using the equation:

$$\%OO_{the} = \left[\frac{IV_0/2A_I}{100+(IV_0/2A_I)\cdot A_0}\right] \cdot A_0 \cdot 100\%. \quad (1.3)$$

In Equation (1.3) A_I and A_0 are the atomic weights of iodine and oxygen respectively and IV_0 is the initial iodine number of the oil used for epoxidation. This value indicates the total grams of iodine necessary to react with all the double bonds present in 100g of oil. To quantify the amount of side reactions, the relative percentage conversion to α-glycol can be used and it is defined as follows:

$$Relative\ conversion\ to\ \alpha - \text{glycol} = \frac{G_{exp}}{G_{the}} \cdot 100\%. \quad (1.4)$$

In Equation (1.4) G_{exp} is the experimentally obtained content of α-glycol and G_{the} is the maximum amount of α-glycol that can be theoretically determined using the equation:

$$G_{the} = \left[\frac{IV_0/2A_I}{100+(IV_0/2A_I)\cdot A_{OH}}\right] \cdot 100\%. \quad (1.5)$$

In Equation (1.5) with A_{0H} is indicated the molecular weight of hydroxyl group. G_{exp} can be determined using the method reported by May (1973). It consists in an oxidation of glycol with benzyl trimethyl ammonium periodate in non-aqueous medium. This method is widely used as suggested by several authors like Dinda *et al*. and Chavan *et al*. [7,8]

On an industrial basis, the process is carried out in large batch reactors in which the oil and carboxylic acid are charged. Afterward the hydrogen peroxide is fed. The time needed to accomplish the reaction is about 8 hours, so high plant investments are needed to obtain enough product with the target quality.

Moreover, this technology shows some safety issues and it is also limited by heat removal, since the reaction is highly exothermic with a standard enthalpy higher than -230 $[kJ/mol]$, especially in the early stages of the reaction [13]. According to Dinda *et al*. and there are four main methods to carry out the epoxidation:

- Epoxidation with peroxycarboxylic acids [9], catalysed by acids or by enzymes [10].
- Epoxidation with organic and inorganic peroxides, catalysed by transition metal catalyst [11].
- Epoxidation halohydrines, with hypohalous acids (HOX) and their salts [9].
- Epoxidation with molecular oxygen using silver as catalyst [9].

This last solution is the cheapest and greenest one but permits to achieve very low yields [7,8]. However, its use is mostly restricted to substrates like ethylene and butadiene owing to very low yields in the case of other alkenes [9,12]. Furthermore, degradation of the oil to low molecular weight volatile compounds such as aldehydes, ketones, and short chains dicarboxylic acids makes the process less selective to epoxide and therefore it is not an efficient method for epoxidation of vegetable oils. Epoxidation using halohydrines is highly environmental unfriendly. Hence, from the above discussion the most industrially used method is the one in which peroxycarboxylic acids are used [7]. Its main advantage of these acids is that they are non-toxic and the by-product is simply water. Also in this work, it is performed an epoxidation with peroxycaarboxylic acids, catalysed by an inorganic acid and conducted in a biphasic system.

It is useful to give a classification of the different epoxidation procedures based on the number of phases of the reaction system:

- Bi-phasic system using carboxylic acid (as a carrier of oxygen) and hydrogen peroxide with or without liquid homogeneous catalyst (inorganic acid);
- Tri-phasic system (organic, inorganic and solid phases) using carboxylic acid (as a carrier of oxygen) and hydrogen peroxide with heterogeneous catalyst (solid).
- Multiphase system exploiting electrochemical reaction with local production of hydrogen peroxide from molecular oxygen. The system is multi-phasic (organic and inorganic liquid phases and a gaseous phase, if one does not consider the two solid electrodes and the exchange-ion membrane).

In the present work, the bi-phasic epoxidation route is followed. In the paragraphs 1.2-1.4 all the main methods presented are briefly discussed, with a particular focus on the bi-phasic one.

1.2 Bi-phasic epoxidation

The reaction occurs in a two-liquid phase system, with interphase mass transfer. In the aqueous phase, carboxylic acid reacts with hydrogen peroxide to produce percarboxylic acid, as of Figure (1.1).

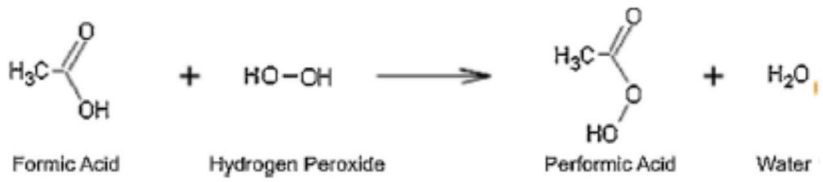

Figure 1.1. Graphical representation of the formation of the peroxycarboxylic acid from hydrogen peroxide and carboxylic acid.

Percarboxylic acid is then transferred to the organic (oily) phase to react with the double bonds of the soybean oil triglyceride molecules, as represented below.

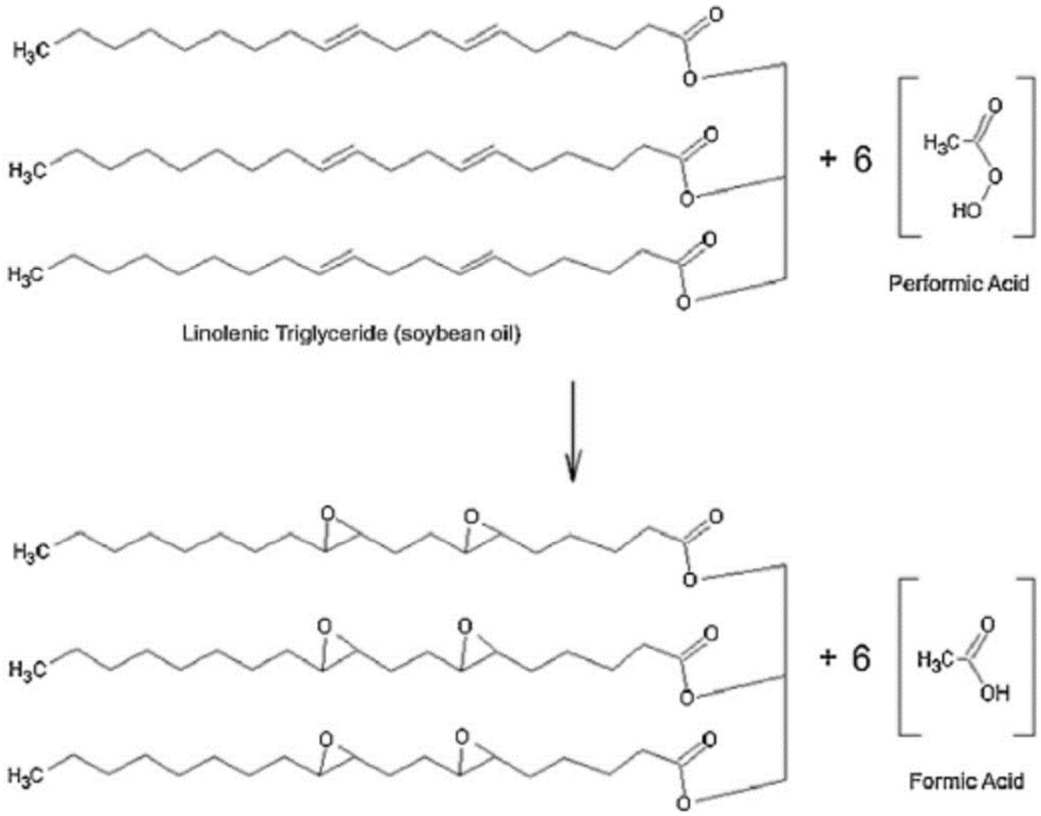

***Figure 1.2**. Graphical representation of a vegetable oil using peroxycarboxylic acid as a carrier of oxygen.*

In this way, the percarboxylic acid transfers the oxygen to the unsaturated oil chains to give the epoxy ring and the carboxylic acid. The mechanism of this reaction involves a bicyclic transition state [34] and can be observed in Figure (1.3).

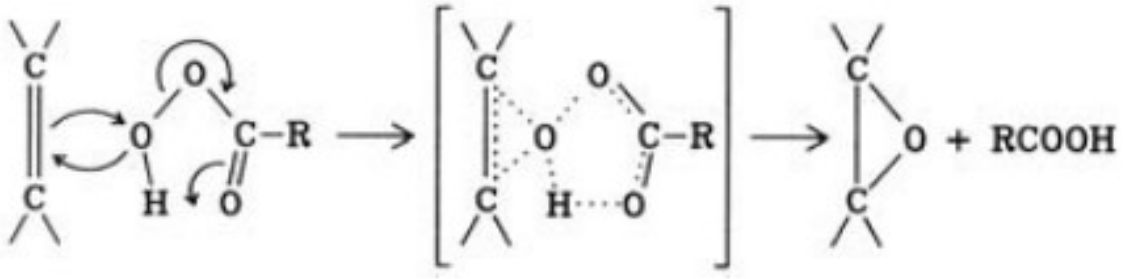

***Figure 1.3**. Mechanism of the epoxidation reaction using peroxycarboxylic acids.*

The resulting carboxylic acid than migrates back to the aqueous phase to be again oxidized by the hydrogen peroxide. The overall process can be represented as of Figure (1.4).

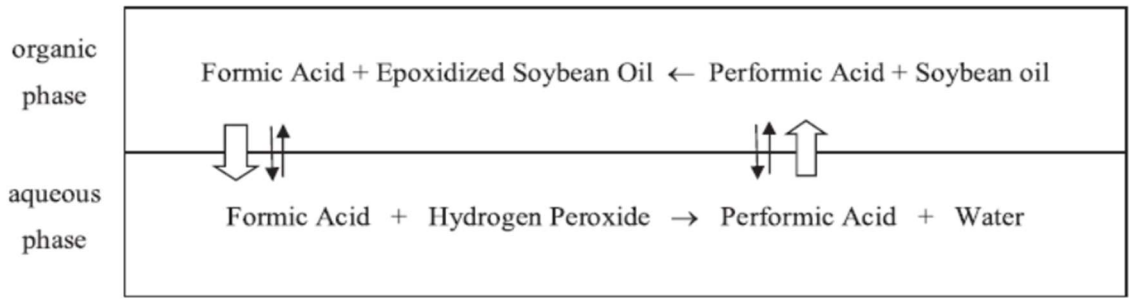

***Figure 1.4**. Schematic representation of the global bi-phasic epoxidation process.*

The reaction cycles between these four steps (two steps of mass transfer between the aqueous and the oily phase, and two reactions, one in each phase bulk), gradually consume hydrogen peroxide in the aqueous phase and the triglyceride double bonds in the oily phase.

As expected, mixing plays an important role in the effective kinetics, as the droplet size depends on the shear, thus on the stirring speed. The magnitude of the interphase contact area and the diffusional layer are thus determined by complex phenomena. Mass transfer is directly affected by the specific surface area. Mixing also plays a key role in the heat transfer between the reaction medium and the cooling system of the reactor. The apparent viscosity of the reaction mixture is determined by droplet size, temperature and stirring velocity. In addition, some by-products are expected like diols and hydroxyl acetate. The side reactions are due to the high reactivity of the epoxy ring. The epoxy ring opening is due to a complex system of reactions but, quite always, only the most relevant one is employed: the cleavage of the oxirane by the oxonium ion [14]. Unfortunately, both the epoxidation of the oil and the cleavage of the oxirane ring are catalysed by acids. Moreover, an excessive use of acids could create problems for a industrialization perspective of this process. In fact, an excessive use of acids besides causing the catalysis of secondary reactions (thus the lowering the oxygen content of the product), leads to much more problems related to the separation and purification of the product. All that

translates into higher operating costs and the achievement of a product with lower commercial value.

1.2.1 Suitability of various inorganic acid catalyst and optimal concentration value

The presence of a liquid inorganic acid catalyst has shown a double beneficial effect on the epoxidation process. At first, according to Zhao *et al*. [15,16] it prevents the spontaneous decomposition of the peroxycarboxylic acid. This aspect promotes the overall epoxidation process stabilizing the oxygen carrier molecule needed to transport the oxygen from the aqueous to the organic phase. Secondly, the presence of an acid prevents the dissociation of the acetic acid. This dissociation would diminish the formation of peroxycarboxylic acid and so the oxirane. Even if this result disagrees with Li *et al*. [5], many authors discuss about the positive effect of acid conditions in the reaction system [2,7,24]. Generally, the suggested pH range is between 3.5 and 6.5. According to Dinda *et al*. [7], both the phosphoric and mainly the sulfuric acid show a great catalytic activity on the process boosting the oxirane formation.

1.2.2 Suitability of various carboxylic acid and optimal concentration value

Acetic and formic acids are widely used as oxygen carrier. Propionic acid can also be used, but its reactivity is weaker [17] and for this reason both acetic and formic acid are preferred. In particular, formic acid shows a fast conversion of the unsaturation of the oil, whereas acetic acid is less reactive. However, formic acid largely promotes the degradation of the oxirane [7]. According to Dinda *et al*. [7], the oxirane conversion is initially higher in the presence of formic acid instead of acetic acid. However, as time progresses, oxirane conversion decreases and iodine value conversion increases gradually using both acids. The course of the oxirane oxygen content with respect to time shows an initial increase until it reaches a maximum value after which it begins to decrease with time. This study shows also that the difference between iodine value conversion and oxirane conversion is higher using formic acid than for acetic acid. This means larger amounts of undesired products with formic acid. Moreover, the latter one is highly corrosive and being more reactive and could lead to excessive rises of temperature including runaway reactions hazard. For these reasons the use of acetic acid is often preferable [2,7,8,18,19]. However, formic acid is still employed by Santacesaria *et al*. [2] and in other few cases [1,17,23]. It is to remind that formic acid promotes the cleavage of the oxirane more than acetic acid. In this study, as oxygen carrier, acetic acid is chosen due to its availability, low price, high epoxidation efficiency and reasonable stability at ordinary operation temperatures [24]. In addition, a crucial role is played by the molar ratio between acid and double-bonds. In

fact, a low concentration of acid limits a good transfer of oxygen to the oil. Conversely, a large amount of acid promotes the formation of by-products. Several authors studied the optimal proportion between acetic acid and ethylenic unsaturation of the oil. According to Dinda *et al*. [7] and Chavan *et al*. [19] this optimum value should be 0.5:1 on a molar basis. Different ratios conduct to the undesired cases earlier discussed, that is a not good transfer of oxygen to the oil or the promotion of epoxy ring opening. Moreover this optimal ratio is also adopted and corroborate by Sniadinovic-Fiser *et al*. [18].

1.2.3 Optimal concentration of hydrogen peroxide

Since the epoxidation rate increases with the concentration of hydrogen peroxide, high concentrations are used to ensure a great reactivity. Dinda *et al*. [7] use hydrogen peroxide at 50% wt., Santacesaria *et al*. [2] and De Quadros *et al*. [1] use hydrogen peroxide at 60%. Higher concentration is adopted by Sepulveda *et al*. [22] (70% and 100%, anhydrous) to demonstrate that the first case is the most effective and some water is necessary to the reaction. It is noticed that at such high concentration of hydrogen peroxide, the danger of explosion is not negligible so for this reason it appears more reasonable to use hydrogen peroxide at lower concentration. In fact, Casson and Maschio [30] investigated the thermal decomposition of hydrogen peroxide at different concentration through a thermal screening unit. From this study the danger of concentrated hydrogen peroxide is evident in fact, the pressure rise due to the decomposition of hydrogen peroxyde at 35%wt is four times higher than lower concentration values. Commercial grade with >35%wt in hydrogen peroxide is available; however, because of the potential risk of detonation for solutions with a hydrogen peroxide concentration of >68%wt, higher grades are potentially far more hazardous and require special care in dedicated storage areas [30]. For this purpose, Jia *et al*. [23], Sinadinovic-Fiser *et al*. [18] use hydrogen peroxide at 30% wt. Moreover, like in the previous case, there is an optimal molar ratio between the hydrogen peroxide and the double-bond of the oil. Dinda *et al*. [7] suggests an optimal molar ratio between 1.5:1 and 2:1. At lower molar ratios, not enough oxygen is available for the epoxidation. Higher amounts of hydrogen peroxide, instead, makes the epoxidized oil less stable, promoting the oxirane cleavage. This ratio is also used by Sinadinovic-Fiser *et al*. [18] and by Chavan *et al*. [19].

1.2.4 Effect of temperature

The process is usually carried out at a temperature within the range of 50°C and 70°C [1,2,7,21,18,19]. On an industrial basis, a temperature of 80°C is generally adopted as a threshold above of which emergency procedure are taken [1]. Because of the side reactions, the temperature cannot be increased too much in order to keep reactions under control. Once reactions are accelerated, an increase in conversion is observed with a decrease in the selectivity

due to the increase of the oxirane cleavage. On the other hand, if the temperature is too low, higher selectivities are obtained but at very low reaction rates thus requiring larger volumes (residence time). For these reasons, most of the authors use a temperature within the range mentioned previously. In fact, Dinda *et al*. [7] investigated the optimal temperature and found the optimum at 60°C, temperature adopted also by Santacesaria *et al*. [2], Leveneur *et al*. [21], Chavan *et al*. [19] and De Quadros *et al*. [1]. A similar result is obtained by Sinadinovic-Fiser *et al*. [18] who found the optimum at 50°C.

1.2.5 Enthalpy of reaction and kinetic parameters

A rigorous study of the enthalpy of both the main reaction and the side one is carried out by Leveneur *et al*. [17] using formic acid as oxygen carrier. According to this study, the enthalpy of the main reaction is equal to -116 kJ/mol whereas the one related to the side reaction is equal to -50 kJ/mol. In order to calculate these enthalpies, mass transfer has not been considered because a kinetic control regime is supposed, thus neglecting mass transfer limitations. However, there is no great clarity about the enthalpy of the main reaction. For example, Santacesaria *et al*. [2] proposed an enthalpy of the main reaction equal to -230 kJ/mol, using formic acid whereas De Quadros *et al*. [1] proposed an enthalpy of this reaction within the range between the two previous values (-196 kJ/mol with formic acid).

As concerns kinetic parameters, Leveneur *et al*. [14] suggests an activation energy value for both reactions equal to 99 kJ/mol and 34 kJ/mol respectively for the main and the side reactions. Similarly, Rangarajan *et al*. [20] calculated values of 76 kJ/mol and 66 kJ/mol respectively. These results are similar, but part of their difference might be related to the molecule used as oxygen carrier. In fact, the first data are obtained using formic acid whereas the second ones are obtained with acetic acid. In the following Table (1.1) these data are summarized.

***Table 1.1**. Thermodynamic and kinetic data of the main and the side reaction.*

	Leveneur *et al.* [14]	**Santacesaria *et al.* [2]**	**De Quadros *et al.* [1]**	**Rangarajan *et al.* [20]**
Type of acid used	formic acid	formic acid	formic acid	acetic acid
$\Delta H_{R,epoxidation}$	-116 kJ/mol	-230 kJ/mol	-196 kJ/mol	-
$\Delta H_{R,degradation}$	-50 kJ/mol	-	-	-
$E_{a,epoxidation}$	99 kJ/mol	-	-	-
$E_{a,epoxidation}$	34 kJ/mol	-	-	-

In conclusion, the typical operating condition according to aforementioned references are summarized below.

***Table 1.2**. Recapitulatory table of the typical process condition of the two-phases epoxidation.*

Temperature	**H_2SO_4 – H_3PO_4 concentration**	**Acetic-formic acid/double bond molar ratio**	**H_2O_2 concentration**	**H_2O_2/double bond molar ratio**	**Time required to maximum yield**
50 – 70°C	0-3% wt	0.5:1	30-60% wt	1.5:1-2:1	6-10h

These operating conditions are taken into account during the experimental procedure dealt in Chapter 3.

1.3 Tri-phasic epoxidation

The process and the reactions are similar to what it was explained in the paragraph 1.2. This route consists in the using a solid acid catalyst instead of a liquid inorganic one. The idea is not so different from the previous route, but it is more complex because of the presence of third a solid phase. The catalysts that are used could be ion exchange sulfonated acid resins or alumina [18,22].

1.3.1 Solid catalyst: ion exchange resin

As regards the ion exchange resins, it is studied by Sinadinovic-Fiser *et al.* [18]. The process is carried out using castor oil, glacial acetic acid and hydrogen peroxide at 30% wt. of concentration and strong cationic exchange resin *Amberlite IR-120*. The authors have tried three different temperatures, 30, 50, 75 °C and the optimum has been found at 50°C.
The acetic acid is preferred with respect to the formic one for the reason about selectivity mentioned in paragraph 1.2. The formation of peroxyacetic acid is catalyzed by ion exchange resin, as confirmed also by Saha *et al.* [33], and the more the catalyst is concentrated the faster is the reaction. Authors have also found that the maximum yield in epoxy content is obtainable in shorter time with greater loading of resin and the maximum yield increases with its loading. The castor oil is diluted with benzene with a 1:1 mass ratio in order to decrease the viscosity of the mixture and to promote the diffusion of the oil in the resin. In addition, the dilution of the organic phase reduces the side reaction of epoxy ring opening. Moreover, the use of a resin as a catalyst instead of the inorganic acid prevents possible polymerization of the acid. The molar ratio between acetic acid and double bond is chosen equal to 0.5, as the previous method.
Hydrogen peroxide at 30% wt. is utilized, with a molar ratio in respect to the double bond of the oil equal to 1.5. The authors have studied also a molar ratio of 1.1 and it was found that increasing the molar ratio from 1.1 to 1.5 implies an increasing of the selectivity. Using molar ratios greater than 1.5 a decreasing of the selectivity is observed because of the epoxy ring opening can easily occur. The catalyst can also be reutilized observing a little decrease on the rate of conversion, on selectivity and the maximum yield decreases with the number of runs. In this way, reutilizing the same catalyst several times requests a greater time to achieve the maximum yield.

1.3.2 Solid catalyst: alumina

This method has been studied by Sepulveda *et al*. [22] and it uses alumina as a solid catalyst exploiting its acid behaviour. The main difference from the previous process consists in the use of ethyl-acetate instead of carboxylic acid. In addition, it is not used virgin oil but its methyl-ester after virgin oil esterification. This route represents an interesting alternative to obtain epoxidized vegetable oil. In particular, methyl oleate and methyl esters of soybean oil are taken into account. It is also employed hydrogen peroxide at 70% wt. of concentration and the process is carried out at 80°C with a massive ratio between oil and catalyst of 5.
Starting from methyl oleate, the authors have tried different kinds of alumina: *Sol-gel*, *Acros* and *Fluka*. The first shows higher values of conversion and it is due to a higher value of surface area per unit of mass with respect to the other ones and the third one the lower. Authors shows also an optimal molar ratio between methyl oleate and hydrogen peroxide of 1:4. The excess of hydrogen peroxide is required because of its partial decomposition is catalysed by the alumina.

In the case of methyl esters of soybean oil epoxidation, *Acros* alumina is used as catalyst.
As regards the reusability of the catalyst, the authors have investigated only *Sol-gel* and *Acros* aluminas. The *Sol-gel* shows a small loss in conversion and a negligible difference in selectivity. On the other side, *Acros* alumina deactivates rapidly showing a prompt loss in conversion from 98% to 50% after three runs.

1.4 Multiphase epoxidation

This particular electrochemical epoxidation is totally different from the other techniques. The epoxide in this case is synthetized in the cathodic and anodic compartments [5]. The main advantage of using this system is the simpler equipment and technological process, a more environmental friendly process easier to control by acting on the current flowing in the cells. The scheme is shown in Figure (1.5).

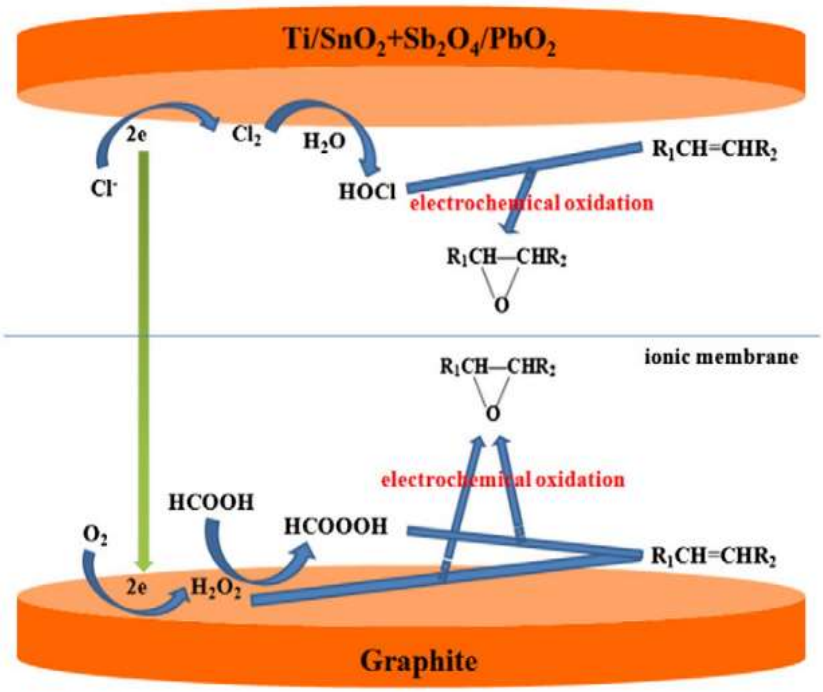

***Figure 1.5**. Schematic representation of the electrochemical epoxidation of unsaturated fatty acids.*

The cell disposed two compartments separated with a cation exchange membrane. The electrodes are made in graphite for the cathode and in $T_i/SnO_2 + S_{b_2}O_4/P_bO_2$ for the anode. In both compartments, the vegetable oil is mixed with the desired carboxylic acid and hydrochloric acid, well mixed and driven to the desired temperature (between 20 and 40°C). With an air bubbler, molecular oxygen is pumped into the cathode at a constant rate of 1 to 5 cm^3/s, generating hydrogen peroxide able to react with the formic acid generating the desired percarboxylic acid which can react with the oil giving the epoxidized product. The molar ratio

between vegetable oil double bonds and formic acid is maintained between 6 and 10. The epoxidation reaction can occur also in the anodic compartment *via* chloridrine [5]. Thanks to the presence of hydrochloric acid, the electrochemical formation of molecular chlorine form chlorine ion is possible. Molecular chlorine can react with water producing chloric and hypochlorous acid. The second one reacts with oil unsaturations producing epoxides. The pH is maintained between 5 and 7 by adding sodium bicarbonate and the epoxidized oil is washed with distilled water and vacuum distilled.

In this way, hydrogen peroxide is not added but it is produced *in situ* by electrochemical synthesis. This is a great advantage form the safety point of view because of the danger of explosion associated with hydrogen peroxide decomposition [30], following this path its production can be finely moduled acting on the current.

Chapter 2
Calorimetric methods and instrumentation

In this chapter the methods and the experimental apparatus for the calorimetric studies are discussed. Reaction calorimetry is a sub-type of calorimetry that is specialized in measuring the energy released or absorbed during the chemical reactions.
Reaction calorimetry is a discipline that allows for thermal and kinetic analysis of a desired process in small scales (e.g. for simulation of failure scenarios purposes), and under realistic conditions (stirring, temperature, pressure, dosing ramps, etc.).

2.1 Calorimetric reactor

The calorimetric reactor used to carry out the epoxidation of the soybean oil consists in a batch, stirred, jacketed and insulated tank designed by *BüchiGlasUster* (Figure 2.1).

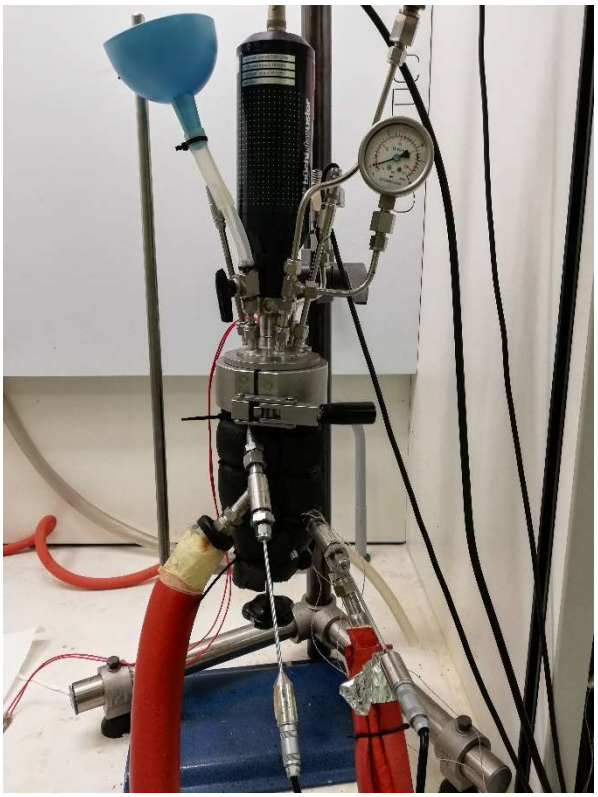

Figure 2.1*. Calorimetric reactor.*

Three PT100 thermocouples record temperature data useful for the calorimetric analysis.
The thermocouples are installed inside the reactor, at the inlet and at the outlet of the jacket. The overall temperature control of the reactor is ensured by a flow of silicone oil in the jacket

and a Huber® thermocryostat in which a specified operative temperature can be set ad accurately controlled. The lateral reactor surface is insulated to minimize heat dissipation to the environment. A sized sketch of the reactor and the impeller is reported in Figure (2.2).

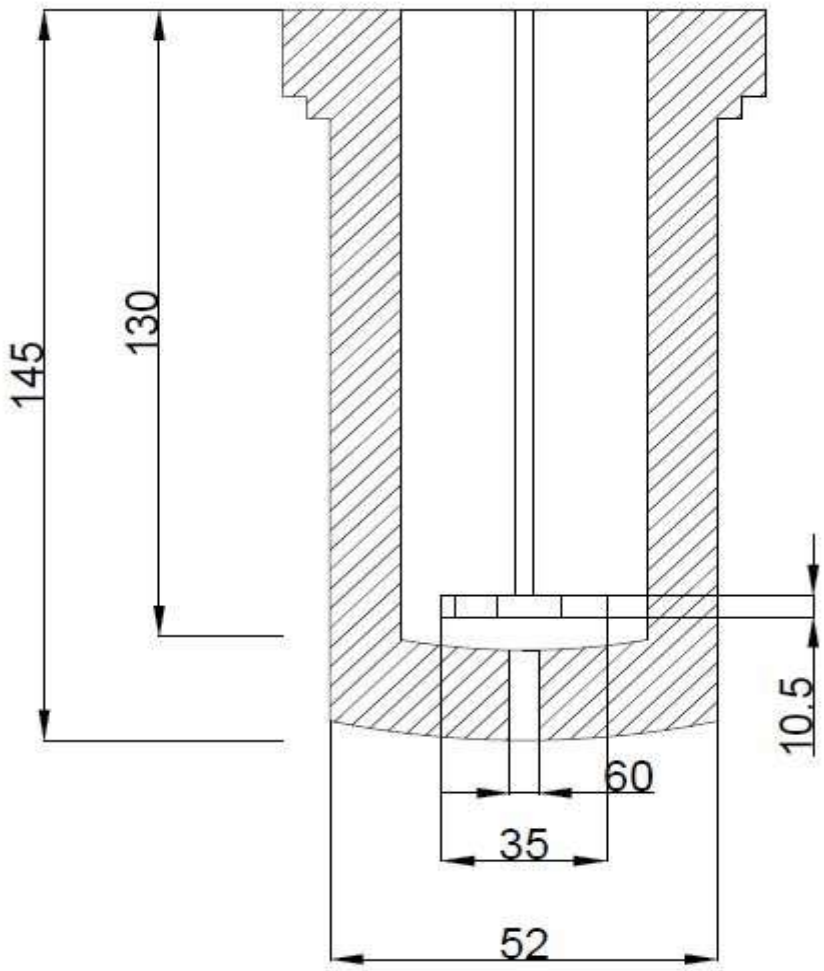

***Figure 2.2**. Sized sketch of a section of the calorimetric reactor. Dimensions in mm.*

A pressure transducer installed in the reactor collects data of the internal pressure. Pressure rises are managed by a rupture disk. Furthermore, an analogic manometer is used to manually monitor the pressure. A stack of electronic ADC (by *National Instrument*®) conveys collected data (pressure and temperature) to the PC via a USB port.

The impeller velocity is governed and data are recorded and visualized thanks to, a LabView NI®-based software. As mentioned before, the calorimetric reactor is also provided with a stirring system used to create a good mixing between the aqueous and the organic phases in order to maximize the interfacial area among these phases. It consists in a 35mm diameter Rushton turbine.

The shaft of the impeller is magnetically coupled to the electric motor, in such a way that sealing is guaranteed. The motor can be controlled either by an electronic interface that permits a fine

regulation by the software, or by a knob on the frontal panel of the interface providing a rough regulation.

2.1.1 Calibration of the stirring system

The stirring system was calibrated to overcome measurement discrepancies between the impeller velocity set using the software and the velocity set manually. A calibration line has been set. A small disk of cardboard with two small slits located at 180° one from each other is fixed on the bottom of the impeller. So, it is placed between the transmitter and the detector of an optocoupler connected to an oscilloscope. The system can be observed in Figure (2.3).

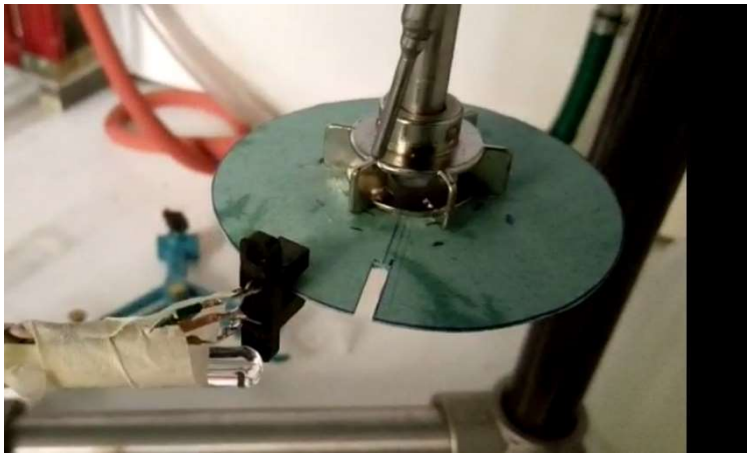

***Figure (2.3)**. Cardboard disk within the optocoupler.*

The employed equipment consists in a manual oscilloscope *HAMEG HM205-3* (Figure 2.4) which allows the observation of varying signal voltages as a two-dimensional plot of one signal as a function of time.

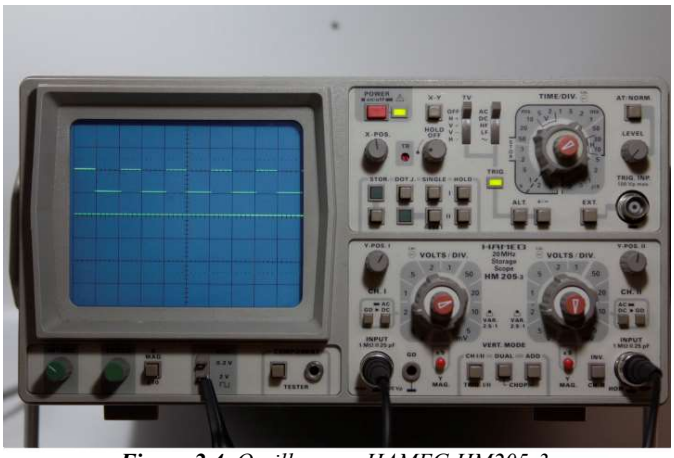

***Figure 2.4**. Oscilloscope HAMEG HM205-3.*

The light signal emitted by the photocell once arrives to its detector is sent as an electrical signal to the oscilloscope. This graphs a continuous profile over a calibrated scale. The observed waveform can be analysed in terms of amplitude, frequency, rise time, time interval, distortion, ….

Once a rotation speed is fixed by sending a specified current to the electric motor, the impeller rotates and the optocoupler gives a peak of the electric signal to the oscilloscope only when one slit cross between the optocoupler led and its detector.

It's noticed that two consecutive peaks (Figure 2.5) do not belong to the same slit so, to get the period of rotation of the impeller, the distance between the first and the third peak had to be considered.

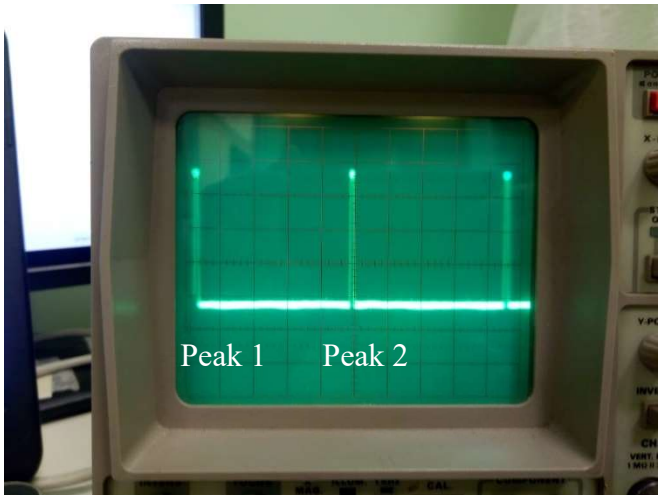

***Figure 2.5**. Signal of the oscilloscope.*

Otherwise, it can be simply observed the number of division from the origin of the x-axis of the oscilloscope and the first peak. In that case that number of divisions is equal to the half of the period. Knowing the electric signal provided to the electric motor, the number of divisions between peaks indicated on the oscilloscope scale and the value of "time per division" chosen in the oscilloscope, it is possible to calculate the revolution per minute of the impeller following the procedure below.

$$T_p = \frac{2 \cdot n \cdot f}{1000}. \tag{2.1}$$

Where with T_p is expressed the period of rotation in seconds, with n the number of divisions in the oscilloscope scale and with f the frequency expressed in $ms/division$.

Knowing the period of the rotation, the speed of revolution is straightforwardly estimated:

$$\omega = \frac{60}{T_p}. \tag{2.2}$$

Whit ω the rotational speed in rpm. The values of speed and the related values of the current intensity is plotted and fitted using MATLAB® as of Figure (2.6).

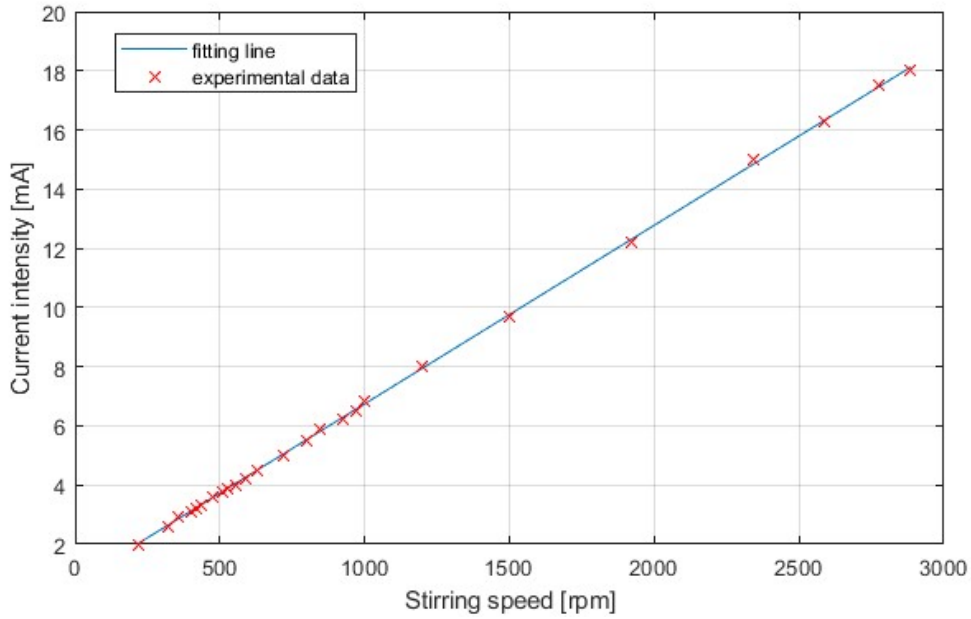

***Figure 2.6**. Plot representing current intensity vs. stirring speed.*

Once the calibration line equation is obtained, it is used in the reactor control software to achieve a fine accuracy in the rotatory speed control.

2.2 Equipment for the determination of the heat exchange coefficient

The heat exchange coefficient was determined by a proper method. Using an electrical ceramic heater (Figure 2.7), a specified thermal power is generated inside the reactor and related temperature variations are recorded. This kind of heater is usually used in 3D printers, it has

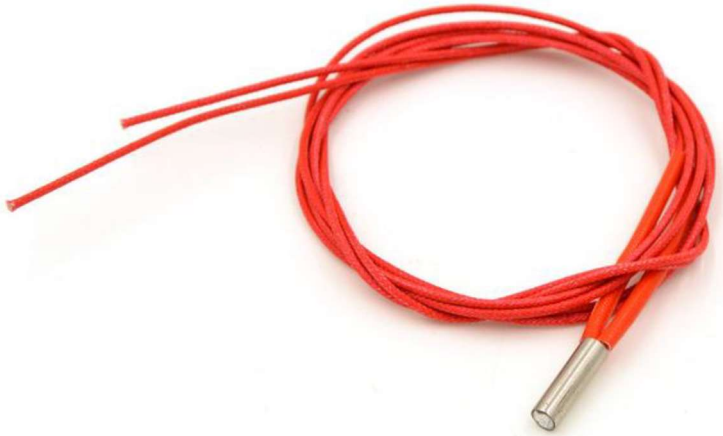

***Figure 2.7**. Ceramic heater used for the determination of the heat exchange coefficient.*

small dimensions (20 mm of length and 6 mm diameter), very low cost, low voltage (24V DC) and good power (40 W nominal) [32].
Different information can be obtained both from the thermal steady state and from the transient. The objective of these measurement is the determination of the power evolved by the sample namely the heat flow, indicated by $\dot{Q}_{flow}$ $[W]$. It can be calculated as follows.

$$\dot{Q}_{flow} = (U \cdot A) \cdot \Delta T. \tag{2.3}$$

In Equation (2.3) ΔT [K] is the measured variable and $U \cdot A$ $[W/K]$ stands for the product between the heat transfer coefficient U $[W/(m^2 \cdot K)]$ and the transfer area A $[m^2]$.
The heat flow can be also calculated through an energy balance on the reactor jacked, as of Equation (2.4).

$$\dot{Q}_{flow} = \dot{m}_j \cdot cp_j \cdot (T_{j,in} - T_{j,out}). \tag{2.4}$$

In Equation (2.4) the measured variables are the temperatures of the cooling fluid at the inlet and at the outlet of the jacked, respectively indicated with $T_{j,in}$ and $T_{j,out}$ [K]. The terms $\dot{m}_j \cdot cp_j$ $[J/K]$ represent the product between the mass flow in the jacket and the heat capacity at constant pressure related to the jacket. The last two terms are calculated through calibration as detailed below.
As regards the steady state, the term $(U \cdot A)$ $[W/K]$ is estimated, as can be seen from Equation (2.3), which applies to the reaction system:

$$Q = U \cdot A \cdot (T - T_j). \tag{2.5}$$

Where T [K] stands for the temperature inside the reactor and T_j [K] for the bulk jacket temperature.
The thermal transient allows instead for the determination of the $(m \cdot cp)$ term. In fact, looking at the shape of the temperature response, the system can be approximated to a first order [32] and the time constant τ can be calculated as follows.

$$\frac{T(t)-T_j}{T(t_0)-T_j} = e^{-\frac{U \cdot A}{m \cdot cp} \cdot (t-t_0)} = e^{\frac{t-t_0}{\tau}}. \tag{2.6}$$

In Equation (2.6) t is the time coordinate and t_0 matches the start of the cooling procedure. The time constant τ is equal to $\frac{U \cdot A}{m \cdot cp}$ and through the term $(U \cdot A)$, $(m \cdot cp)$ is estimated.

The experimental investigation showed that the internal resistance and so the absorbed electrical power can change. In this way, a constant thermal generation can be hard to be achieved and Equation (2.3) should be solved. The problem was avoided by changing the generated power. In this way, its influence on the heat exchange coefficient is readily investigated. Variations in

the generated power were finely and automatically achieved by means of a platform called *Genuino* (*Arduino*) as of Figure (2.8).

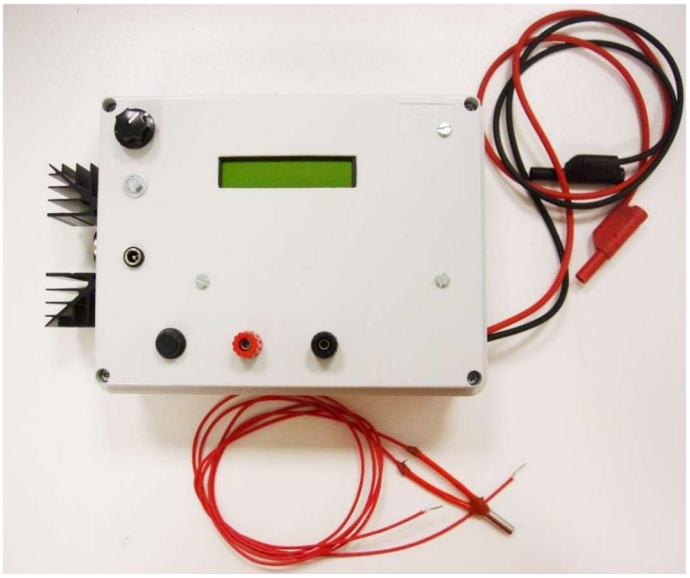

Figure 2.8 *Automatic power controller and ceramic heater.*

The control is achieved using a feedback controller, the measured instant power applied to the resistor is compared with the value of the power set-point. The microcontroller *ATmega 328* adjusts the voltage applied to the resistor on the base of the difference between the instant power and the set point power value permitting to control the power with a precision of about 1-3%.

Chapter 3
Materials and methods

This chapter is focused on the experimental procedure used for the experiments and on the employed materials. Firstly, a list of all the materials used in the reaction step, the separation and the purification are listed. Then, the methods required to carry out the experiments is illustrated.
It is reminded that, in the present work, acetic acid is used instead of formic acid even if it is less reactive. In this way the risk of corrosion of the instrumentations is reduced. Moreover, hydrogen peroxide at 35%wt is used instead of the more common 60%wt [1,2,13,22]. This choice implies weaker reaction conditions but also a safer process reducing the risk of detonation or runaway [29,30].

3.1 Materials

Reactants used in the experimental investigation are listed below:

- Soybean oil in a food grade, from a local supermarket (*Despar*);
- Acetic acid 98% (*Dow chemicals*);
- Hydrogen peroxide 35%wt (*Alfa Aesar*);
- Sulfuric acid 98.5% (*Sigma-Aldrich*);
- Sodium hydrogencarbonate 99% (*Alfa Aesar*);
- Diethyl ether 98% (*Alfa Aesar*);
- Hydrobromic acid 33%wt (*Alfa Aesar*);
- Potassium phthalate 99% (*Alfa Aesar*);
- Crystal violet as pH indicator.

3.2 Experimental procedures

In this paragraph, the calibration of the calorimetric reactor, the epoxidation process, the product separation and purification and the purified product analysis steps are explained.

3.2.1 Calibration of the calorimetric reactor

The heat exchange coefficient of the calorimetric reactor is determined through a set thermal power generated in the reactor (see paragraph 3.4). The calorimetric reactor is filled with 45g

of soybean oil, 37.3g of hydrogen peroxide and 6.695g of acetic acid. It is noticed that no catalyst, i.e. sulfuric acid, is added. In this way, the epoxidation is avoided during the calibration step and thus a correct calculation of the heat exchange coefficient because no enthalpy of reaction is released. In order to perform a calculation of the heat exchange coefficient in a way as accurate as possible, it is important to use the same reaction mixture of the process in such a way the overall system is the same as it is during the epoxidation process.
The electric terminals of the ceramic heater are properly insulated with a sealant and are finally introduced in the reactor. The chosen temperature is set to the Huber® thermocryostat and a time equal to about 40 minutes must be elapsed to obtain the thermal steady state of the system and so to allow the calibration procedure Calibrations have been performed, at the three operative reaction temperatures (40°C, 55°C, 70°C), and a fixed value of the impeller speed (500rpm). Once the heater is connected to the automatic power controller, the power is set. For each temperature, different powers are used: 5W, 10W, 15W, 20W, 25W. After the application of a power value to the resistor, a new thermal steady state is reached. Before proceeding, the system is allowed to cool down until the primal steady state. The system reaches the steady state in about 15-20 minutes, depending on the temperature at which the calibration is performed. The data of temperature, as mentioned before (paragraph 2.1), are collected by three thermocouples located in the reactor, at the inlet and at the outlet of the jacked, respectively. Temperature data are elaborated using a proper algorithm build in *Matlab*®. The following table collects the times required to the stationary states following the heating and the cooling steps.

***Table 3.1**. Times required to the thermal steady state following a heating-cooling process to the initial steady state.*

Temperature [°C]	Heating time [min]	Cooling time [min]
40	15	15
55	15	20
70	15	15

These times are required to bring the system at a thermal stationary state after the providing of the thermal power, and to bring it at the initial thermal stationary state once the power is removed.

3.3 Epoxidation in the calorimetric reactor

The epoxidation is carried out using 45g of soybean oil, a ratio between hydrogen peroxide and double bonds equal to 0.5:1, a ratio between acetic acid and double bonds equal to 1.5:1 and an amount of sulfuric acid equal to 3% on a mass basis with respect to the oil.
Quantities are determined from the double bonds concentration of the soybean oil. As mentioned in Chapter 1, this value is expressed through the iodine number. All samples of oil used in the experimental tests were analysed by *3A Laboratori s.r.l.*, an accredited laboratory. The iodine number values are reported in Table (3.2).

***Table 3.2**. Iodine number values related to the oil utilized.*

Sample	**Iodine number** $\left[\frac{g_{I_2}}{100 g_{oil}}\right]$
1	122.7
2	128.7
Mean value	125.7

The oil iodine number allows for the determination of the double bonds concentration:

$$N_{I_2} = \frac{IV_0}{MW_{I_2}}. \tag{3.1}$$

N_{I_2} stands for the moles of iodine needed to react with all the double bonds in 100g of oil.
Given the stoichiometry between unsaturations and iodine which is 1:1, it can be stated that the number of moles of iodine needed to react with 100g of oil, are also equal to the number of moles of double bonds contained in 100g of oil. Thus, the moles of double bonds in 45g of oil is given by Equation (3.2):

$$N_{\mathrm{C=C}} = \frac{N_{I_2} \cdot 45}{100}. \tag{3.2}$$

From the mass and the density of the soybean oil, the concentration of double bonds is expressed in Equation (3.3).

$$C_{\mathrm{C=C}} = \frac{N_{\mathrm{C=C}} \cdot \hat{\rho}_{oil}}{m_{oil}}. \tag{3.3}$$

In Equation (3.3) $\hat{\rho}_{oil}$ expresses the mass density of soybean oil and it is equal to $0.917 \cdot 10^3\ g/l$ [31]; m_{oil} represents the mass of the oil $[g]$.

From this value all reactant quantities are determined and are summarized in Table (3.3).

Table 3.3. *Reactant quantities utilized in the calorimetric reactor.*

Reactant	Reactant-double bonds ratio	Mass [g]
Soybean oil	-	45
Acetic acid	0.5:1	7.695
Hydrogen peroxyde	1.5:1	37.305
Sulfuric acid	0.06:1	1.351

The desired operative temperatures are firstly set using the *Huber* thermocryostat. The desired amount of soybean oil is weighted using an analytical balance by *Acculab*® and it is transferred into the reactor until the jacked temperatures reach the steady state. The reactor control software is launched and the desired impeller velocity is set. At this point the acetic acid and hydrogen peroxide are weighted and transferred in the reactor. Less than 10g of mixture is put aside and inserted in the reactor later. This sequence in the reactants add is justified by two reasons. Firstable, in order to obtain a well stable mixture which means good mixing, it is observed experimentally that the oil must be added, heated and stirred before the adding of the aqueous phase. After some minutes also acetic acid and hydrogen peroxide can be added. Following this procedure, the discharged mixture at the end of the reactor runs remains stable otherwise, the mixture would de-mix in a couple of minutes compared to about 10 minutes if this addition order is followed. Moreover, the thermocouple inside the reactor is located 4mm above the impeller and so, to ensure a proper measure, it must be fully covered by the liquid. This means that a minimum height of liquid inside the reactor must be guaranteed to have the real value of temperature and to check the thermal steady state. For this reason, all the reactants apart from the sulfuric acid have to be put inside the reactor to ensure a proper temperature measurement. Finally, when the thermal steady state is reached, the sulfuric acid is added to the remaining 10g of mixture and finally transferred inside the reactor. Since the sulfuric acid amount is very little, it is preferred to weight it in a becher where are still present the 10g of mixture to limit the amount of acid sticked to the becher walls. At this point the reaction is considered to be initiated.

Once the experimental timing is fulfilled, the temperature data acquisition and the impeller are stopped from the control software. At this point the mixture reacted can be discharged in a becher through a manual valve located at the bottom of the reactor. The two phases form a stable mixture and they must be separated in order to avoid the oxirane cleavage and to ensure a correct result in the following analysis.

3.3.1 Epoxidized soybean oil separation and purification

The becher with the reaction mixture is quenched using cold water to stop, or at least slow down, the ongoing reactions. After that, the mixture is transferred into a separatory funnel to perform a liquid-liquid extraction to separate the organic and the aqueous phase. Before the separation, a neutralization step is performed to suppress the system acidity to avoid the oxirane cleavage (§1.2). The neutralization is realized with three washings using a 0.2M solution of sodium hydrogen carbonate. One washing consists in adding the sodium hydrogen carbonate to the solution in the separatory funnel with the reaction mixture. The funnel is plugged and then shaked to maximize the contact between the reaction mixture and the neutralizing solution. The mixture then separates into an upper organic and a lower aqueous phase. At this point the aqueous phase is discharged and the following washing is performed. The procedure is the same for the first two washings. In the last one, before discharging the aqueous phase, the neutrality is checked prior to the ESBO analysis. After the shaking of the separatory funnel, a pH indicator is thus introduced to read the pH of the mixture. If the pH is equal to 7 the aqueous phase is discharged and the organic one is transferred to a test tube. On the contrary, an additional washing is required. Traces of diethyl ether are added to speed up the de-mixing process and to avoid water traces in the organic phase. This solvent shows a great affinity with the epoxidized oil, so they form a unique phase from which the remaining water traces suspended in the oil precipitates downward.

At this point the sample contented in the test tube, in addition to ESBO, also contain diethyl ether added to eliminate all the water. It must be extracted to perform a correct analysis of the product. Indeed, by weighting the sample before this operation, the weight of the sample would be overestimated.

This is performed by connecting the test tube to a vacuum pump by *KNF* (provided also with a vacuum flask) to enhance the volatility of the diethyl ether. The ether tends to evaporate and to be stored in the vacuum flask. The evaporation process is enhanced by slightly shaking the vial and by heating it up in a thermostatic bath (*Julabo*®) kept at 55°C. Once all the ether is removed, the sample is stored at low temperature (4°C) in the fridge and it can be analysed.

3.3.2 Epoxidized soybean oil analysis

As exposed in Chapter 1, the soybean oil conversion is quantified from the determination of the oxirane oxygen content in the epoxidized soybean oil. The determination is carried out using the American Oil Chemists' Society (AOCS) official method Cd 9-57 [25]. This is realized through a titration with a solution of hydrobromic acid in acetic acid with the following procedure.

Firstly, it is necessary to titrate the hydrobromic acid solution in order to assess its exact title. This operation is needed because in ambient condition hydrobromic acid is gaseous tending to lower the solution concentration through evaporative processes. A quantity equal to 0.4000g of potassium phthalate is weighted and dissolved in a becher with 10ml of acetic acid. A magnetic stirrer is introduced and a heating plate with magnetic agitation (*IKA RCT*) is used to help the solubilization. After the complete solubilization, four drops of the indicator (crystal violet) are introduced and the becher is covered using parafilm to avoid hydrobromic acid breakaways. The final part of a burette filled of hydrobromic acid solution is then inserted in the becher through the parafilm. Hydrobromic acid is gradually added until the colour of the potassium phthalate turns from violet to light green. At this point the equivalents of the bromidic acid used are equal to the potassium phthalate equivalents. The solution title is readily calculated starting from the volume used to ensure the equivalence and the mass of the titrated potassium phthalate mass:

$$N_{HBr} = \frac{m_{ph}}{0.2042 \cdot V_{HBr}}. \tag{3.4}$$

In Equation (3.4) N_{HBr} $[eq/l]$ stands for the normality of hydrobromic acid, m_{ph} for the phthalate mass [g] and V_{HBr} for the volume of hydrobromic acid used to reach the equivalence point.

Once the exact title of the hydrobromic acid solution is known, the content of oxirane oxygen in the ESBO can be determined. A mass of 0.3g of ESBO is weighted and solubilized in 10ml of acetic acid. After the adding of four drops of crystal violet and a magnetic stirrer, the ESBO is titrated using the hydrobromic acid solution with the same methodology. Finally, the oxirane oxygen content (expressed as grams of oxirane oxygen per grams of epoxidized oil) can be calculated as:

$$\%OO = \frac{1.6 \cdot V_{HBr} \cdot N_{HBr}}{m_{ESBO}}. \tag{3.5}$$

In Equation (3.5) $\%OO$ is the oxirane oxygen content $[\%]$ and m_{ESBO} the mass of the ESBO sample titrated $[g]$.

Afterwards, the ESBO sample is also analysed by FTIR spectroscopy.

3.4 Determination of the heat exchange coefficient of the calorimetric reactor

The method applied to determine the heat exchange coefficient, mentioned in Chapter 2, is analysed in detail in this section.
A well determined thermal power is generated inside the reactor and pertinent temperature variations are recorded. Both from the thermal steady state and from the transient, different information are obtained. Taking into consideration the cooling transient and approximating the system to a first order, it is also possible to estimate the time constant τ.
This time constant is equal to $(m \cdot cp)/(U \cdot A)$ as can be seen from the Equation (3.6):

$$\frac{T(t)-T_j}{T(t_0)-T_j} = e^{-\frac{U \cdot A}{m \cdot cp} \cdot (t-t_0)} = e^{-\frac{t-t_0}{\tau}}. \tag{3.6}$$

Where $(U \cdot A)$ is the global heat exchange coefficient $[W/K]$, $(m \cdot cp)$ is the thermal capacity of the mixture inside the reactor $[J/K]$ and t_0 refers to the cooling starts.
This model can be rigorously derived from the heat balance of the batch reactor during the cooling considering the liquid as incompressible and the absence of chemical reactions:

$$m \cdot cp \cdot \frac{dT}{dt} = -U \cdot A \cdot (T - T_j). \tag{3.7}$$

The Equation (3.7) can be rearranged giving:

$$\frac{dT}{T-T_j} = -\frac{U \cdot A}{m \cdot cp} \cdot dt. \tag{3.8}$$

A proper integration of this equation gives the Equation (3.6).
As regards the steady state, it is possible to determine $(U \cdot A)$ knowing the thermal power applied through the heater, the temperatures of the jacket and the one related to the reactor as can be observed from the Equation (3.9):

$$Q = U \cdot A \cdot (T - T_j). \tag{3.9}$$

In this way, it is possible to obtain information about the terms $(U \cdot A)$.

3.4.1 Study of the cooling transient: heat transfer coefficient

The determination of τ is obtained from the cooling transient by passing to logarithms:

$$\ln\big(T(t) - T_j\big) = -\frac{U \cdot A}{m \cdot cp} \cdot (t - t_0) + \ln\big(T(t_0) - T_j\big) =$$

$$= -\frac{t-t_0}{\tau} + \ln\big(T(t_0) - T_j\big). \tag{3.10}$$

In this form, Equation (3.10) has the shape of a straight-line, in fact it can be wrote as follows:

$$y = -\frac{1}{\tau}x + b. \tag{3.11}$$

Once different thermal powers are imposed (Chapter 2), the collected temperature data are elaborated and the instantaneous difference $T(t) - T_j = \Delta T(t)$ is obtained. T is the internal reactor and T_j the jacket temperature. $\ln\left(T(t) - T_j\right)$ is then calculated and a linear fitting is performed. This procedure is applied for each different value of thermal power: 5W, 10W, 15W, 20W and 25W. An exemplificative test (at 70°C) is represented in Figure (3.1).

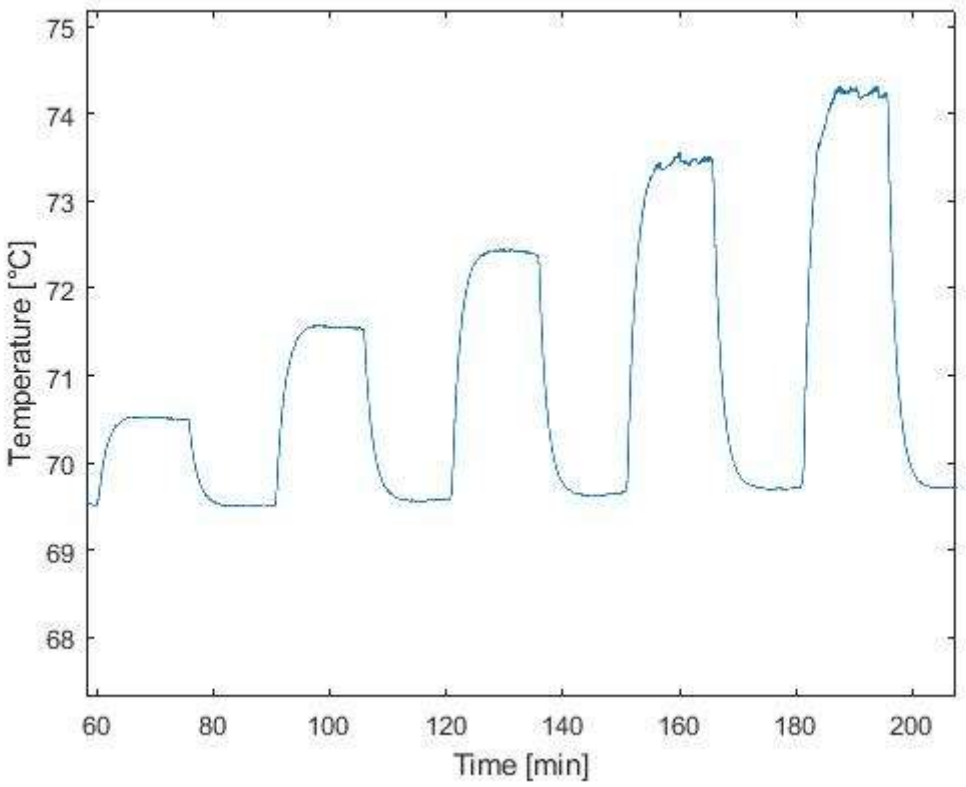

***Figure 3.1**. Time evolution of the temperature setting a thermal power of 5W, 10W, 15W, 20W and 25W at 70°C.*

Each transient is analysed and fitted at all three temperatures considered. In Figure (3.2) the fitting done on the transient at 70°C after the application of 5W of thermal power is reported:

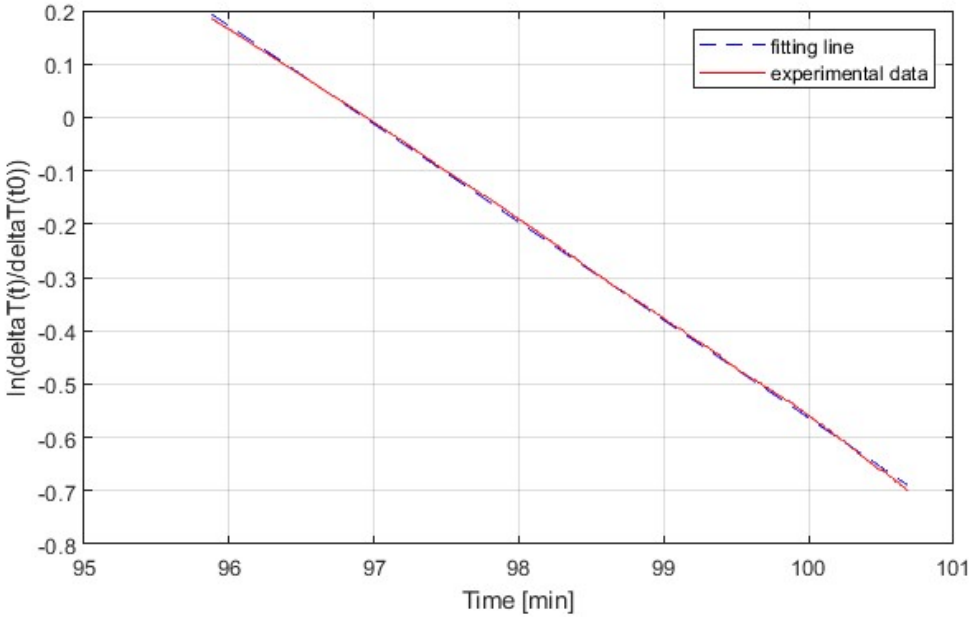

***Figure 3.2**. Logarithm of ΔT(t) (blue) and its fitting (red) in the test at 70°C using a power of 5W.*

In these tests, the reactor is loaded with the same reactants quantities used for the epoxidation and at the same operating conditions (temperature, impeller velocity).
Concerning the fitting at 40°C, 55°C and 70°C the values of τ are respectively 0.1644, 0.1995 and 0.1953 min^{-1}. A result summary is reported in Table (3.4)-(3.6).

***Table 3.4**. Values of the parameters obtained by fitting data using power of 5, 10, 15, 20, 25W.Reactor temperature of 40°C.*

Temperature [°C]	**Power [W]**	**τ^{-1}[min^{-1}]**	**τ[min]**	**$\tau^{-1}[s^{-1}] = \frac{U \cdot A}{m \cdot cp}$**	**$\tau[s] = \frac{m \cdot cp}{U \cdot A}$**
	5	0.1840	5.435	0.003066	326.116
	10	0.1573	6.359	0.002621	381.557
40	15	0.1591	6.284	0.002652	377.013
	20	0.1612	6.203	0.002687	372.165
	25	0.1604	6.235	0.002673	374.079
Mean value		**0.1644**	**6.103**	**0.002740**	**366.1**

***Table 3.5**. Values of the parameters obtained by fitting data using power of 5, 10, 15, 20, 25W. Reactor temperature of 55°C.*

Temperature [°C]	Power [W]	τ^{-1}[min^{-1}]	τ[min]	$\tau^{-1}[s^{-1}] = \frac{U \cdot A}{m \cdot cp}$	$\tau[s] = \frac{m \cdot cp}{U \cdot A}$
	5	0.2074	4.822	0.003456	289.314
	10	0.2000	4.999	0.003337	299.690
55	15	0.1965	5.088	0.003275	305.381
	20	0.1935	5.1673	0.003225	310.036
	25	0.2000	5.000	0.03333	300.016
Mean value		**0.1995**	**5.015**	**0.003325**	**300.8**

***Table 3.6**. Values of the parameters obtained by fitting data using power of 5, 10, 15, 20, 25W. Reactor temperature of 70°C.*

Temperature [°C]	Power [W]	τ^{-1}[min^{-1}]	τ[min]	$\tau^{-1}[s^{-1}] = \frac{U \cdot A}{m \cdot cp}$	$\tau[s] = \frac{m \cdot cp}{U \cdot A}$
	5	0.1838	5.441	0.003063	326.432
	10	0.2078	4.812	0.003464	288.699
70	15	0.1952	5.123	0.003253	307.388
	20	0.1920	5.208	0.003200	312.470
	25	0.1979	5.052	0.003299	303.137
Mean value		**0.1953**	**5.127**	**0.003256**	**307.6**

R^2 coefficients are greater than 0.997 in each test and so the fitting quality is acceptable.
In conclusion, the mean values of 366.1, 300.8 and 307.6 seconds are found for 40, 55 and 70°C respectively. This value is linked to the time spent for the transient depletion that amounts to 4-5τ, that is 12-27 minutes on average. It is noticed that the time constant determined at 40°C is considerably greater than that pertaining to 55 and 70°C. Since this time constant represent the ratio between the heat capacity of the system and its heat transfer capacity, a decreasing of this ratio with temperature is reasonable because a smaller temperature means more thermal inertia. Increasing the temperature what is observed is the decreasing of the thermal inertia contribution with respect to the heat transfer capacity of the system.

3.4.2 Study of the steady state: heat transfer coefficient

Data obtained with 5, 10, 15, 20 and 25W are considered in the steady state thermal study that was applied to three aforementioned temperatures (40, 55 and 70 °C). The test methodology and operative conditions were kept unchanged as for the transient study. Using Equation (3.9) ($U \cdot A$) is obtained and also the power dissipated Q_d [W] by the system. Rearranging Equation (3.9):

$$T = \frac{Q}{U \cdot A} + T_j = \frac{P - Q_d}{U \cdot A} + T_j. \tag{3.12}$$

The results are summarized in Table 3.7.

Table 3.7*. Values of heat transfer coefficient ($U \cdot A$) and dissipated power Qd for each temperature.*

Temperature [°C]	$\mathbf{U \cdot A}\left[\frac{W}{K}\right]$	$\mathbf{Q_d}$ [W]
40	2.215	0.801
55	2.866	0.878
70	2.770	0.730
Mean value	2.617	0.803

From this table it can be noticed that the values of the heat exchange coefficient ($U \cdot A$) determined at 55 and 70°C (performing tests at different power values) are comparable, showing a difference of 3.3% so not substantial differences are noticed. Whereas, at 40°C the value of the global heat exchange coefficient results to be much smaller with a difference of 20% and 22% compared to the values at 55°C and 70°C respectively. Results of the cooling transient in Table (3.4)-(3.6) are in line with stationary data. From the obtained values of the heat transfer coefficient, rising the temperature, an increasing trend can be observed.
In addition, it is reminded that the value of ($U \cdot A$) could be determined also from the value of $(U \cdot A)/(m \cdot cp)$ (par. 3.4.1), since the value of ($m \cdot cp$) of the mixture is known.
This simplified approach may lack accuracy because of the (neglected) presence of the impeller inside the reactor with its contribution to the total heat capacity. In addition, this approach does not consider the value of the heat losses from the reactor sections that are not insulated. Otherwise, with the employed approach, ($U \cdot A$) is computed at steady state and so, knowing the value of this parameter and the time constant τ determined in the cooling transient, it is possible to determine also ($m \cdot cp$) value. It is important to be noticed that this value of ($m \cdot cp$)

is not the theoretical one but the effective one, since its value is related to the overall system (including also the thermal capacity of the impeller and the heat losses).

3.5 Determination of the heat of the process

Since the global heat transfer coefficient $(U \cdot A)$ is well known at each process temperature (par. 3.4), the total heat of the reaction set of the process can be estimated. The temperature profiles of the three longest rector runs (one associated at each process temperature) are integrated in *Matlab* after steady state temperature is subtracted. The integration is performed by trapezoidal integration from the instant the reaction starts (considered when the sulfuric acid is added to the reaction mixture) to the end of the reaction which are 7, 15 and 25 hours for 70, 55 and 40°C respectively. In order to get the enthalpy associated at the overall process in kJ/mol a complete double bonds conversion is considered. Since in the reactor $45g$ of oil are loaded, the total number of double bonds is 0.2228 mol. The obtained results are summarized in Table (3.8).

***Table 3.8**. Total thermal power generated during the epoxidation process.*

Temperature [°C]	$\boldsymbol{\Delta H_{tot}}\left[\frac{kJ}{mol}\right]$
40	-292
55	-266
70	-215
Mean value	-258

These obtained values are in line with the literature ones [2,13].

Chapter 4
Isothermal reactor modelling

The literature suggests several approaches to the isothermal modelling of the considered reactive system. Two main possibilities are discussed: the detailed biphasic model and the simplified pseudo-homogeneous model. The latter simplifies the effective kinetics description and overlooks the complex mass transfer issues.

4.1 Epoxidation reactor modelling approaches

4.1.1 Pseudo-homogeneous model

As reported before, it can be assumed that the epoxidation process takes place in a single pseudo-phase (i.e., pseudo—homogeneous system). This assumption considers a unique phase whose properties are averaged on the constituent phases (oil and aqueous).
This assumption simplifies the kinetic model and avoid the use of the distribution coefficients for the quantification of the different species in the aqueous and oil phases. In addition, interphase mass transfer contributions are neglected since no interfaces are considered. Practically, this approach matches a system with a very high agitation rate in which transfer limitations are minimized. High rotational speeds of the mixing equipment favour the formation of small drops in the aqueous phase, increasing the external surface for mass transfer and minimizing limitations to the mass transfer [24]. Under those assumptions, the mass transfer is thus neglected intrinsically assuming a global kinetic control of the process.
As it can be seen from the literature [24], this approach is equivalent to think the system made of elementary reactions.

4.1.2 Multiphase model with interphase mass transfer

A multiphase model is more detailed than the pseudo-homogeneous approach, especially in what dealing with the kinetics and the mass transfer description. In this case, the system is composed by two partially miscible phases. For sake of simplicity Figure (1.3) is reported below.

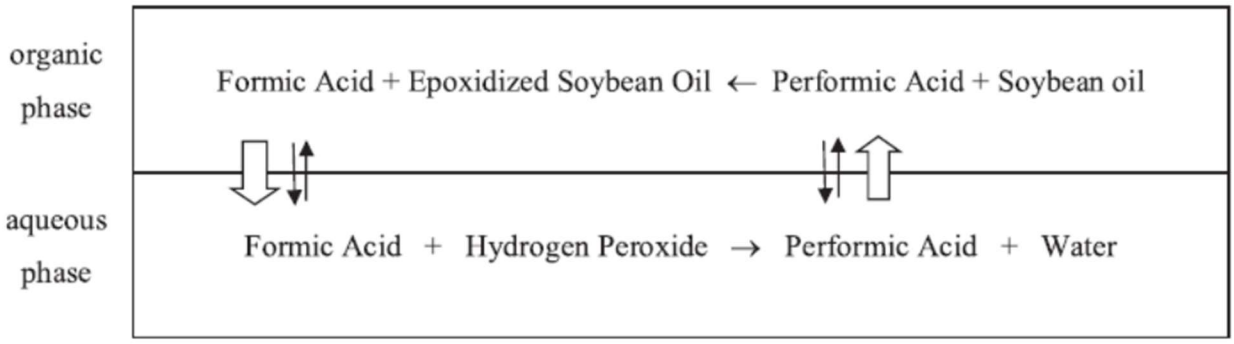

***Figure 1.3**. Schematic representation of the global bi-phasic epoxidation process.*

Between there is an interface across which chemical species migrate from a phase to the other feeding the chemical reactions. In fact, as mentioned in Chapter 1, the main reaction occurs between the unsaturations of the soybean oil (organic phase) and an atom of oxygen of the hydrogen peroxide through peracetic acid (aqueous phase). It is clear that epoxidation of the oil is admitted only if peracetic acid migrates from the aqueous phase to the organic one. On the other side, the epoxidation reaction produces acetic acid, which instead must migrate from the organic phase to the aqueous one to react with hydrogen peroxide to peracetic acid. This continuous migration sustains the epoxidation. It is noticed that the concentration of a generic species is higher in the bulk of the phase in which the particular species is more soluble. The general trend is represented in Figure (4.2).

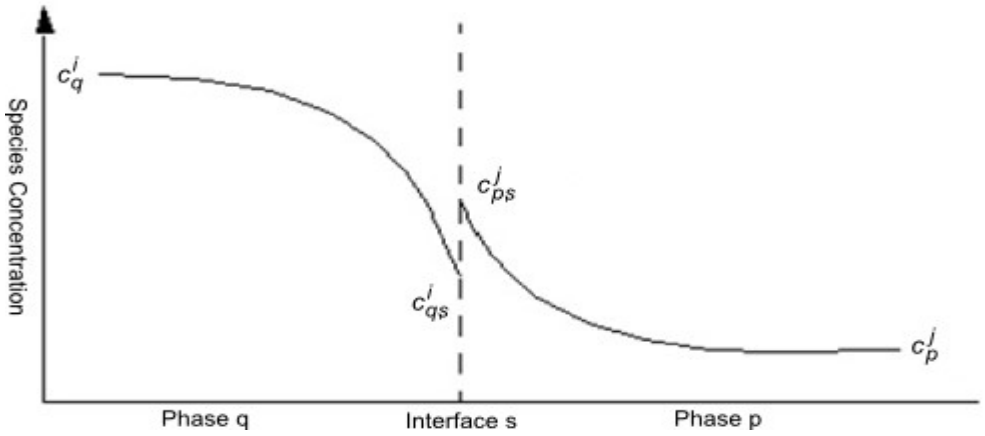

***Figure 4.2**. Concentration trend of the generic species "i" among generic phases "p" and "q".*

The discontinuity in the correspondence of the interface "s" is due to the different affinity each species has with respectively the two phases.

4.2 Conceptual modelling of the experimental apparatus

The experimental apparatus is composed by the calorimetric reactor in which reactants are loaded prior to the reaction start. Products (and unreacted reagents) are then discharged at the

end of the reaction. So, the epoxidation is carried out in a batch reactor. The Table (4.1) gives the framework of the quantities of all reactants utilized.

***Table 4.1**. Summarizing table of all reactants quantities.*

Reactant	Mass [g]
Soybean oil	45
Acetic acid	7.695
Hydrogen peroxyde	37.305
Sulfuric acid	1.351

As mentioned in Chapter 3, the quantities of acetic acid, hydrogen peroxide and sulphuric acid depend on the amount of soybean oil. In addition, to have a proper temperature measurement, the mass of oil is chosen in such a way to ensure a total height of liquid almost equal to the diameter of the reactor. Doing this, the thermocouple inside the reactor is fully submersed and so the measured temperature can be considered representative of that of the mass bulk of the reaction system. It is reported the reaction system schematization in Figure (2.2).

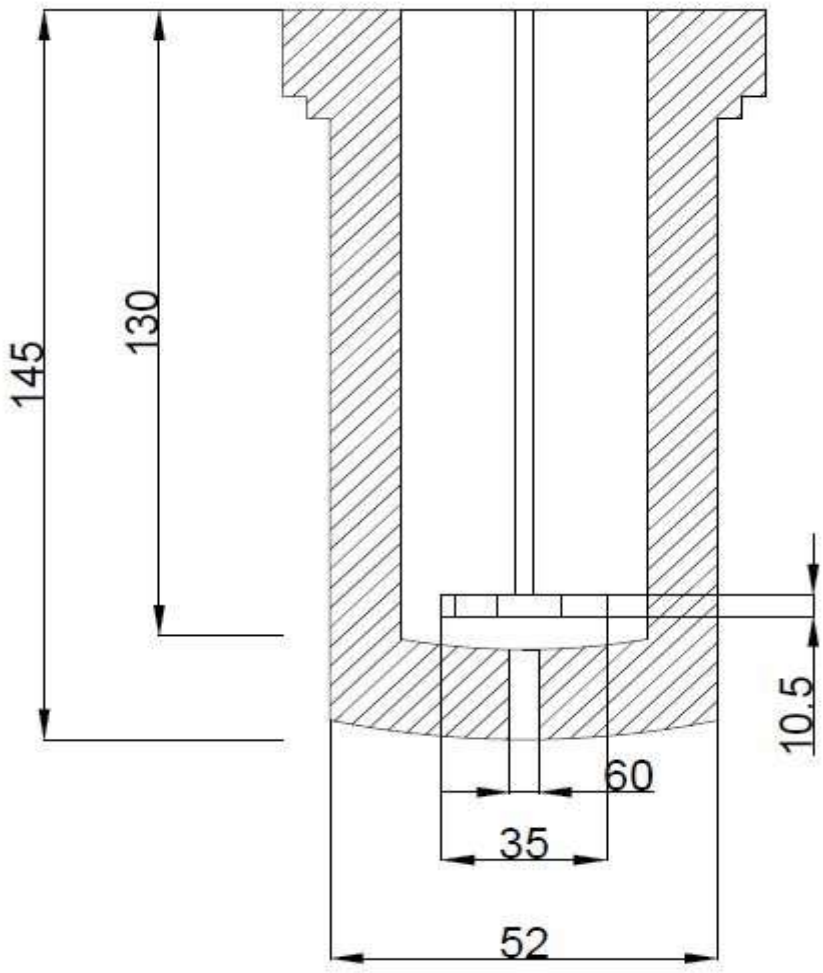

***Figure 2.2**. Sized sketch of a section of the calorimetric reactor. Dimensions in mm.*

The quantities of the employed reactants allow to respect the proportions between the total liquid height and the diameter of the calorimetric reactor.

4.3 Isothermal reactor modelling

4.3.1 Relevant balances, model assumptions and hypothesis

The generic mass balance for a batch reactor is developed starting from the generic balance definition:

$$A = IN - OUT + P - C. \tag{4.1}$$

A stands for the accumulation term, *IN* for the mass inputs, *OUT* for the mass outputs, and *P* for the production term and *C* the consumption.

By definition, in a batch reactor inputs and outputs are discarded leading to the simplified balance:

$$A = P - C. \tag{4.2}$$

The instantaneous molar formulations for a generic species *j* is reported in Eq. (4.3):

$$\frac{dN_j}{dt} = V \cdot \sum_n^{i=1} \cdot v_{ij} \cdot r_i. \tag{4.3}$$

Where, $\frac{dN_j}{dt}$ represents the variation of the number of moles of species *j* over time, *V* is the volume of the liquid, v_{ij} the stochiometric coefficient of species *j* in the reaction *i* and r_i the rate of the *i-th* reaction.

The reaction system is very complex because of the high reactivity of epoxide groups produced which can bring to a wide range of secondary reactions and related sub-products. According to the literature [2], it is reasonable to assume only two epoxide degradation reactions producing glycols. In fact, the epoxides can react with almost all involved chemical species giving glycols. As proven by Santacesaria *et al*. considering all the possible epoxide ring opening reactions or a unique degradation reaction, the kinetic runs shows comparable results [2]. For this reason, only the reaction between epoxy ring and acetic and peracetic acid is considered. As regards the peracetic acid formation reaction, it is considered as a reversible reaction otherwise, all the other ones, can be considered as irreversible [2,7,24,3].

The considered reactions are:

- The production of peracetic acid (reversible);
- the degradation of hydrogen peroxyde (irreversible);
- the epoxidation reaction (irreversible);
- the degradation of epoxy ring reacting with acetic acid (irreversible);
- the degradation of epoxy ring reacting with peracetic acid (irreversible).

Furthermore, it must be pointed out that the reaction between the double bonds and the peracetic acid (epoxidation reaction, according to La Scala and Wool [27] occurs with rates that are different for trienes, dienes or monomers respectively. In particular, La Scala and Wool [27] demonstrated that trienes are much more reactive than dienes and monomers, and perhaps also the ring opening reaction rate would be susceptible to the characteristic of the molecular structure. In this work, this aspect is not considered because no information on the oil molecular composition is available. The oil is therefore considered as homogeneous. For this reason, within which the kinetic constants estimated by the model all the contributes related to all monomers, dienes and trienes are indistinctly present.

Being the system biphasic, each reaction can theoretically occur in both phases. However, literature surveys showed that some reactions are negligible in specific phases because of the

tendency to take place only in one phase [2,7,14,24,27]. So, it is necessary to perform the mass balances on both phases. The specific reaction system is illustrated below.
Reactions considered in the aqueous phase are:

1) direct reaction of production of peracetic acid;
2) inverse reaction:

$$H_2O_2 + CH_3COOH \underset{k1,k2}{\longleftrightarrow} CH_3COOOH + H_2O. \tag{4.4}$$

3) Degradation of hydrogen peroxide:

$$H_2O_2 \overset{k3}{\rightarrow} H_2O + \frac{1}{2}\, O_2. \tag{4.5}$$

The kinetic system in the organic phase is instead given by:

4) Epoxidation reaction:

$$C = C + CH_3COOOH \overset{k4}{\rightarrow} \quad COC + CH_3COOH. \tag{4.6}$$

5) Degradation of the epoxy ring due to the acetic acid:

$$COC + CH_3COOH \overset{k5}{\rightarrow} \quad C - C - OH. \tag{4.7}$$

6) Degradation of the epoxy ring due to the peracetic acid:

$$COC + CH_3COOOH \overset{k6}{\rightarrow} C - C - OH. \tag{4.8}$$

For sake of simplicity, from now on, on the balances the acetic acid is indicated with “AA”, hydrogen peroxide with “HP”, peracetic acid with “PAA”, the unsaturation of soybean oil with “C=C”, epoxy groups with “EP”, water with “W” and glycols with “EG”. Furthermore, only the shift of some species among the two phases is allowed. This assumption is based on the partition coefficient of the species, defined as:

$$K_j = \frac{C_j^w}{C_j^o}. \tag{4.9}$$

In Equation (4.9) C_j^w $[mol/l]$ is the molar concentration of the generic species *j* in the aqueous phase and C_j^o $[mol/l]$ the molar concentration of the *j* species in the organic phase.
According to several authors like Leveneur *et. al.* the partition coefficient of soybean oil, epoxidized soybean oil and glycols can be assumed almost equal to zero, while those of the hydrogen peroxide and water are considered very large [2,14]. This means that hydrogen peroxide and water are found exclusively in the aqueous phase while soybean oil, epoxidized soybean oil and glycols, are found only in the organic phase. For this reason, the interphase shift is considered only for acetic acid and peracetic acid. The partition coefficient of these two

species are estimated using the cubic equation of state Soave Redlich Kwong coupled with the semi-empirical UNIFAC approach. In Table 4.2 the partition coefficients K_j are summarized for all the species.

***Table 4.2**. Partition coefficient K_j of main species involved in the epoxidation process.*

Chemical species	**K_j [-]**
AA	3.8
PAA	27.0
HP	$\rightarrow \infty$
C=C	$\rightarrow 0$
EP	$\rightarrow 0$
W	$\rightarrow \infty$
EG	$\rightarrow 0$

Mass balances for each system's constituent and based on the two phases are summarized below:

Aqueous phase:

$$\frac{dN_j^w}{dt} = V^w \cdot \left(-J_j^w \cdot \sum_n^{i=1} \cdot \upsilon_{ij} \cdot r_i\right). \tag{4.10}$$

Organic phase:

$$\frac{dN_j^o}{dt} = V^o \cdot \left(-J_j^o \cdot \sum_n^{i=1} \cdot \upsilon_{ij} \cdot r_i\right). \tag{4.11}$$

The mass transfer rate per unit of volume of the generic species j is indicated with $J_j^{w;o}$ $[mol/(l \cdot min)]$.

The apex *w* is referred to the aqueous phase, while *o* stands for the organic phase. This mass transfer rate is considered positive from the aqueous phase to the organic one. The mass transfer phenomena are described by the Whitman's two film theory. For this reason, all concentration gradients are confined into the boundary layers of the two liquid sides [28].

The balances are expressed in terms of concentration, reminding that the moles can be expressed as the product between the volume and the pertaining concentration:

$$\frac{d(V \cdot C_j)}{dt} = V \cdot \frac{d(C_j)}{dt} + C_j \cdot \frac{d(V)}{dt} = V \cdot \sum_n^{i=1} \cdot v_{ij} \cdot r_i. \quad (4.12)$$

Under the assumption of constant volume, since the derivative of the volume is equal to zero, the contribute of the volume can be simplified from the equation.
Under this assumption, the reaction system is the following.
Aqueous phase:

$$\frac{dC_{AA}^{w}}{dt} = -r_1 + r_2 - J_{AA}^{w}. \quad (4.13)$$

$$\frac{dC_{H_2O_2}^{w}}{dt} = -r_3. \quad (4.14)$$

$$\frac{dC_{PAA}^{w}}{dt} = r_1 - r_2 - J_{PAA}^{w}. \quad (4.15)$$

$$\frac{dC_{H_2O}^{w}}{dt} = r_3. \quad (4.16)$$

Organic phase:

$$\frac{dC_{AA}^{o}}{dt} = r_4 + J_{AA}^{o}. \quad (4.17)$$

$$\frac{dC_{PAA}^{o}}{dt} = -r_4 + J_{PAA}^{o}. \quad (4.18)$$

$$\frac{dC_{C=C}^{o}}{dt} = -r_4. \quad (4.19)$$

$$\frac{dC_{EP}^{o}}{dt} = r_4 - r_5. \quad (4.20)$$

$$\frac{dC_{EG}^{o}}{dt} = r_5 + r_6. \quad (4.21)$$

The overall system, for the considered reaction system, is assumed to be isothermal and so, no energy balances coupling is required.

4.3.2 Kinetic equations

The reacting system is made of two partially miscible phases. The water phase is polar while the oil system can be assumed nonpolar. Hydrogen peroxide reacts in the aqueous phase with acetic acid (AA) to give PAA, which in turn reacts in the organic phase through a combination with the double bonds (C=C) of the unsaturated fatty acid chains to form the epoxy (EP) ring together with AA. The latter then goes back to the aqueous phase to feed the ‘oxygen-shuttling’

cycle. In the literature there are no clear and univocal references about the kinetic of the reactions of peracetic acid production and the epoxidation of the oil [2,26]. For this reason, those reaction are assumed as elementary reaction. So, related kinetics are the product between the kinetic constant and the reactants concentration. Moreover, the peracetic acid production is a reversible reaction, it is possible to calculate the kinetic constant of the inverse reaction knowing the equilibrium constant of the reaction since it is defined as follows:

$$K_{1,eq} = \frac{\vec{k}_1}{\overleftarrow{k}_1}. \tag{4.22}$$

Therefore, rearranging the Equation (4.22), the kinetic constant of the inverse reaction $\overleftarrow{k}_1$ can be expressed as a function of the kinetic constant of the direct reaction $\vec{k}_1$ (indicated in the balances simply as k_1) knowing the value of the equilibrium constant $K_{1,eq}$ which is equal to 5.17 [2] as can be observed in Equation (4.23).

$$\overleftarrow{k}_1 = \frac{\vec{k}_1}{K_{1,eq}}. \tag{4.23}$$

The kinetic expression related to the hydrogen peroxide decomposition considers instead a 2.5 order as Santacesaria *et al*. have demonstrated [2,26].

$$r_1 = k_1 \cdot C_{AA}^{w} \cdot C_{HP}^{w}. \tag{4.24}$$

$$r_2 = \frac{k_1}{K_{1,eq}} \cdot C_{PAA}^{w} \cdot C_{W}^{w}. \tag{4.25}$$

$$r_3 = k_3 \cdot (C_{HP}^{w})^{2.5}. \tag{4.26}$$

$$r_4 = k_4 \cdot C_{C=C}^{o} \cdot C_{PAA}^{o}. \tag{4.27}$$

$$r_5 = k_5 \cdot C_{EP}^{o} \cdot C_{AA}^{o}. \tag{4.28}$$

$$r_6 = k_6 \cdot C_{EP}^{o} \cdot C_{PAA}^{o}. \tag{4.29}$$

Furthermore, it is assumed that all these considered reactions takes place only in the bulk of the respective phase, and not at the interphase.

4.3.3 Mass transfer modelling approach

The mass transfer rate for the component *j* in the phase *i* is indicated with J_j^i $[mol/(l \cdot min)]$ and it is defined according to the Whitman's two film theory as:

$$J_j^i = \beta_j^i \cdot \left(C_j^{i,b} - C_j^{i,i}\right). \tag{4.30}$$

Where $C_j^{i,b}$ stands for the concentration $[mol/l]$ of species *j* in the phase *i* in the bulk, $C_j^{i,i}$ represents the concentration $[mol/l]$ of species *j* in the phase *i* at the interphase and β_j^i is defined as follows:

$$\beta_j^i = h_{m,j}^i \cdot A^{wo}. \tag{4.31}$$

β_j^i $[1/min]$ is the product between $h_{m,j}^i$, namely the mass transfer coefficient of species *j* in the phase *i* $[1/(min \cdot m^2)]$ and the interfacial area A^{wo} between the aqueous and the organic phase $[m^2]$. It gives an indication to the mass transfer efficiency.
According to the definition of partition coefficient K_j given before, the interfacial concentrations of the species at the interphase can be expressed as:

$$C_j^{w,i} = K_j \cdot C_j^{o,i}. \tag{4.32}$$

And so, the mass transfer rates for acetic acid and peracetic acid are:

$$J_{AA}^w = \beta_{AA}^w \cdot \left(C_{AA}^{w,b} - K_{AA} \cdot C_{AA}^{o,i}\right). \tag{4.33}$$

$$J_{PAA}^w = \beta_{PAA}^w \cdot \left(C_{PAA}^{w,b} - K_{PAA} \cdot C_{PAA}^{o,i}\right). \tag{4.34}$$

$$J_{AA}^o = \beta_{AA}^o \cdot \left(C_{AA}^{o,i} - C_{AA}^{o,b}\right). \tag{4.35}$$

$$J_{PAA}^o = \beta_{PAA}^o \cdot \left(C_{PAA}^{o,i} - C_{PAA}^{o,b}\right). \tag{4.36}$$

Interfacial concentrations are readily obtained once the following constraints, that holds at steady state conditions, is ensured:

$$V^w \cdot J_j^w = V^o \cdot J_j^o. \tag{4.37}$$

Consequently, the following expression for the interphase concentrations can be derived:

$$C_{AA}^{o,i} = \frac{V^o \cdot \beta_{AA}^o \cdot C_{AA}^{o,b} + V^w \cdot \beta_{AA}^w \cdot C_{AA}^{w,b}}{V^w \cdot \beta_{AA}^w \cdot K_{AA} + V^o \cdot \beta_{AA}^o}. \tag{4.38}$$

$$C_{PAA}^{o,i} = \frac{V^o \cdot \beta_{PAA}^o \cdot C_{PAA}^{o,b} + V^w \cdot \beta_{PAA}^w \cdot C_{PAA}^{w,b}}{V^w \cdot \beta_{PAA}^w \cdot K_{PAA} + V^o \cdot \beta_{PAA}^o}. \tag{4.39}$$

For sake of simplicity, the two β_i^w are considered as equal, as the two β_i^o are. This simplification appears reasonable because of acetic and peracetic acid are chemically very similar so their mass transfer coefficients too. In addition, according to the definition of β_i given in Equation (4.29), the other contribute to it is given by the interfacial area A^{wo} which is a physical property of the reaction system, so it does not vary depending on the substance.

4.4 Results and discussion

Through the developed model, starting from the experimental data obtained as mentioned in Chapter 3, the determination of the kinetic and mass transfer parameters is possible.
This model permits to determine the optimal parameter values which implies the minimum error between the experimental epoxide concentrations and the calculated ones. The error (Err) is express as the mean squared error as presented in Equation (4.40).

$$Err = \sum \left(C_{EP}^{experimental} - C_{EP}^{calculated}\right)^2. \tag{4.40}$$

In particular, the optimized parameters are all the kinetic constants (k_1, k_2, k_3, k_4, k_5, k_6) and the product between the mass transfer coefficient and the interfacial area associated at each phase (β^w, β^o). To perform the model, it is necessarily first set the initial concentrations presented in Table (4.3) noticing that the volume of the organic phase is equal to $4.91 \cdot 10^{-2}$ l and the aqueous phase one is $4.21 \cdot 10^{-2}$ l.

***Table 4.3**. Initial concentrations of the reaction system.*

Substance	Concentration [mol/l]
Acetic acid in water phase	3.13
Hydrogen peroxide	9.38
Peracetic acid in water phase	0
Water	32.90
Double bonds	4.54
Epoxidized soybean oil	0
Acetic acid in organic phase	0
Peracetic acid in organic phase	0

In the model, it is analyzed the evolution along the reaction time, of the individual species at each phase: the acetic acid, hydrogen peroxide, peracetic acid and water in the aqueous phase and the soybean oil, epoxidized soybean oil, acetic acid and peracetic acid in the organic phase.

The concentrations profiles obtained from the *Matlab* simulation are presented at each process temperature in Figure (4.4)-(4.6):

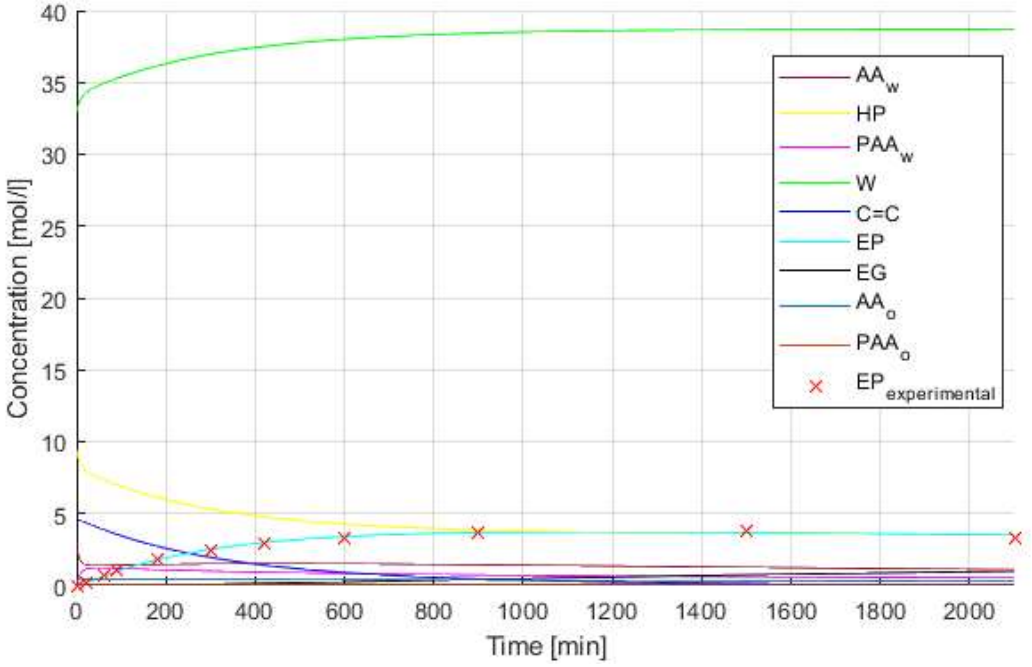

Figure 4.4. *Concentration profiles with respect to time for the simulation at 40° C.*

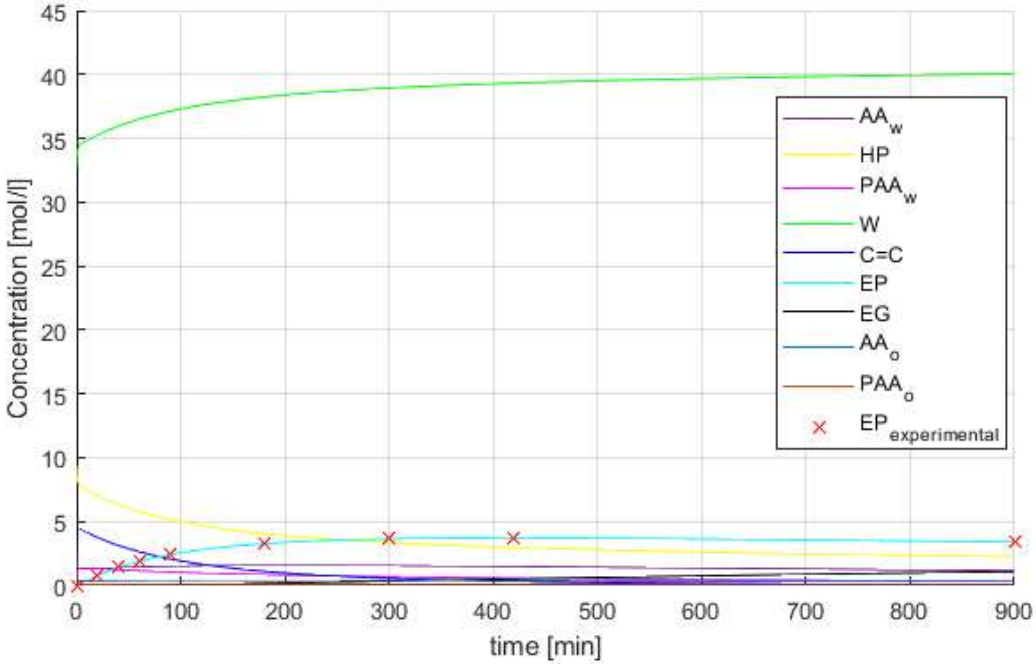

Figure 4.5. *Concentration profiles with respect to time for the simulation at 55° C.*

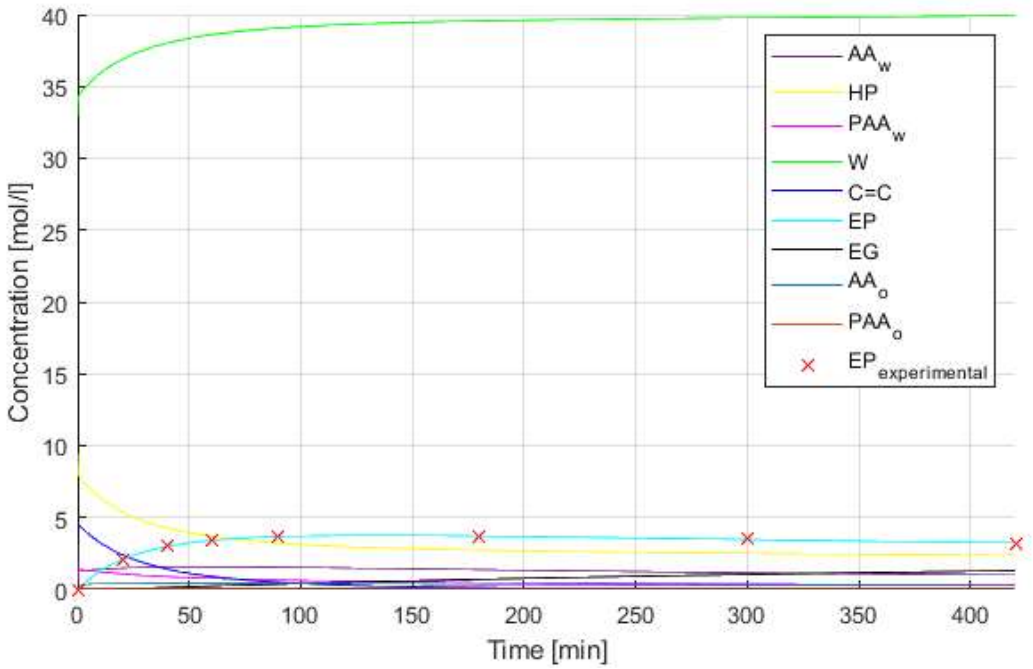

***Figure 4.6**. Concentration profiles with respect to time for the simulation at 70° C.*

Experimentally, the highest oxirane oxygen content found is 6.617%, achieved operating at 40°C after 15 hours. According to Equation (1.2) this means a relative conversion to oxirane equal to 85% since from Equation (1.3) the theoretical maximum oxirane oxygen that can be theoretically obtained is 7.88%. Although this value is obtained at 40°C, it is recommended to conduct the reaction at higher temperatures to reduce drastically the time required to achieve relative conversion values of the 80%. As it can be observed by the previous figures, the experimental values are well fitted by the model. In Table (4.4) R^2 factors for each simulation are reported.

***Table 4.4**. R^2 coefficient values for each simulation.*

Temperature [°C]	R^2 [-]
40	0.996
55	0.999
70	0.999

At 40°C the consumption of double bonds is the slowest compared to the other temperatures. The concentration of the acetic and peracetic acid in the organic phase is almost zero. The first

one reacts rapidly with the double bonds of the soybean oil or with the epoxy ring causing its degradation; the second one, or it is transferred into the aqueous phase or it is reacted with the oxirane ring, degrading it and generating glycols.

At 55°C, it is possible to visualize at the last stages a decrease in the concentration of the epoxides, led by the degradation. The concentration of acetic and peracetic acid in the organic phase is practically zero.

At 70°C the double bonds are consumed faster than other temperatures. Also, at this temperature, the degradation is emphasized more than the other temperatures. In fact, the concentration of epoxides decreases at earlier stages with respect to the profiles at 40°C and 55°C. Again, the concentration of acetic and peracetic and in the organic phase is practically zero. At each temperature, the concentration of water increases with time. Its increase is greater at higher temperatures and it is due to the degradation of the hydrogen peroxide and to the reaction of peracetic acid formation (Equation (4.4)-(4.5)). This implies a progressive dilution of the system during the epoxidation process. As regards double bonds, they are not consumed entirely. The maximum double bonds conversion is observed at 70°C after 7 hours, with a value of 99.8%. Although the experimental data at this temperature are taken up to 7 hours, while at 40°C and 55°C there is a data collection up to 15 and 35 hours respectively, this value of conversion in never reached at the lower temperatures even if the conversion is almost total anyway. At longer time, at each temperature, the glycols concentration increases implying a diminishing of epoxides concentration and so a loss in selectivity. This phenomenon is observed earlier at higher temperatures.

As mentioned before, from these three simulations the kinetic constant and resistance to mass transfer coefficient values are determined and are reported in Table (4.5).

***Table 4.5**. Parameter values determined by the model.*

Parameter	T=40°C	T=55°C	T=70°C	Unit
k_1	$6.49 \cdot 10^{-3}$	$4.94 \cdot 10^{-2}$	0.286	$l/(mol \cdot min)$
k_3	$5.25 \cdot 10^{-17}$	$4.57 \cdot 10^{-6}$	$1.71 \cdot 10^{-4}$	$l^{1.5}/(mol^{1.5} \cdot min)$
k_4	$8.38 \cdot 10^{-2}$	0.212	0.765	$l/(mol \cdot min)$
k_5	$2.99 \cdot 10^{-22}$	$3.49 \cdot 10^{-4}$	$5.51 \cdot 10^{-6}$	$l/(mol \cdot min)$
k_6	$5.83 \cdot 10^{-3}$	$9.69 \cdot 10^{-3}$	$4.91 \cdot 10^{-2}$	$l/(mol \cdot min)$
β^w	$8.82 \cdot 10^{-2}$	1.99	2.35	$1/min$
β^o	3.33	19.28	59.60	$1/min$

As expected, the values of both kinetic constants and resistance to the mass transfer increases with increasing temperature.

Looking at the kinetic constant values, the epoxides degradation is mainly imputable to the effect of the peracetic acid because of the kinetic constant (k_4) associated to the reaction between epoxides and acetic acid is several orders of magnitude smaller than the one related to the peracetic (k_5).

It is noticed that the developed model considers all the reaction (except r_3) as elementary ones. So, all the consideration are based on this simplify reaction system.

As concern the epoxidation reaction, having calculated values of its kinetic constant based on experimental data at three different temperatures, an estimation of the pre-exponential factor and of the activation energy is possible using the Arrhenius equation:

$$k = A \cdot e^{-\frac{E_a}{R \cdot T}}. \tag{4.41}$$

In Equation (4.41) A $[kJ/mol]$ is the pre-exponential factor and E_a the activation energy $[kJ/mol]$. Taking the natural logarithm of the Arrhenius equation yelds:

$$\ln(k) = -\frac{E_a}{R} \cdot \left(\frac{1}{T}\right) + \ln(A). \tag{4.42}$$

This has the same form as an equation for a straight line and allow to fit the three values of the kinetic constant as it can be seen from Figure (4.7).

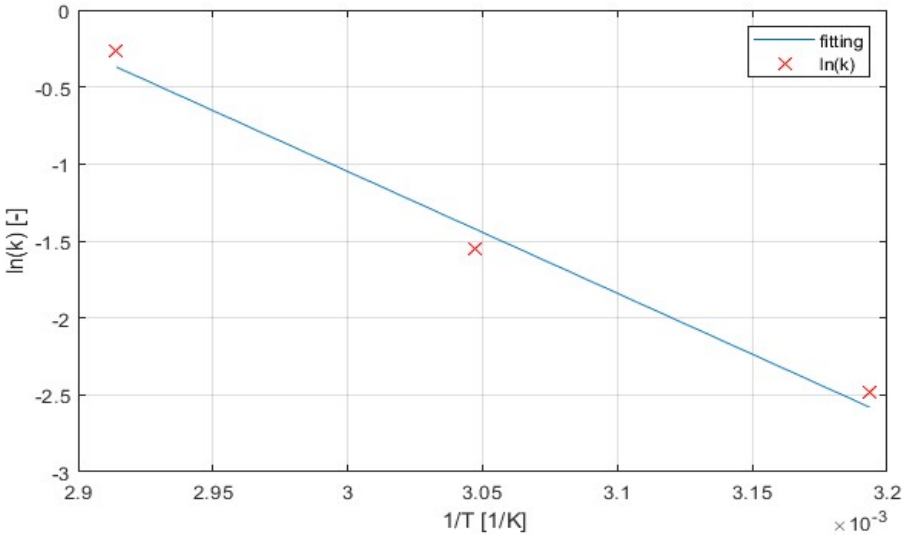

***Figure 4.7**. Arrhenius plot for epoxidation of soybean oil by peroxyacetic acid.*

From the previous plot, the following results are obtained:

***Table 4.6**. Pre-exponential factor and activation energy values for the soybean oil epoxidation reaction.*

A $[kJ/mol]$	E_a $[kJ/mol]$
$7.16 \cdot 10^6$	65.79

The obtained values are in line with the literature [14].

It is noticed a huge difference between the mass transfer efficiency associated with the aqueous phase with respect to the one related to the organic phase. In fact, β^o is greater than β^w of some orders of magnitude. This is not attributable to interfacial area A^{wo} because it has the same value among the two terms but to a more efficient transport mechanism into the organic interfacial layer.

If the temperature rises, both the mass transfer efficiency increase. This is due to an increasing of both terms which compose those parameters: A^{wo} and h_m^i. Temperature could promote the formation of smaller droplets and so an increasing of the interfacial surface. In fact, at higher temperatures, the coalescence phenomena are reduced [35]. Anyway, it is more reasonable a major impact of the temperature on the mass transfer coefficient. Comparing the magnitude of the increasing of the two mass transfer parameters, the one related to the water layer remains almost constant with respect to the one associated to the organic layer. This could be due to a less sensitivity of the water physical properties to the temperature. Anyway, these difference between the two mass transfer efficiency parameter is not relevant to the overall process

because looking at Figures (4.8)-(4.10) mass transfer is never the rate determining step of the process.

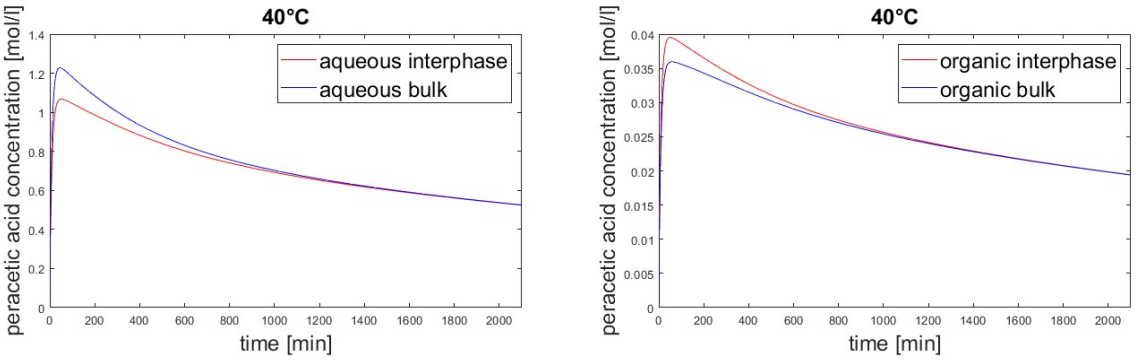

***Figure 4.8**. Time evolution of peracetic acid concentrations at the interphase and in the bulk of both organic and aqueous phase at 40°C.*

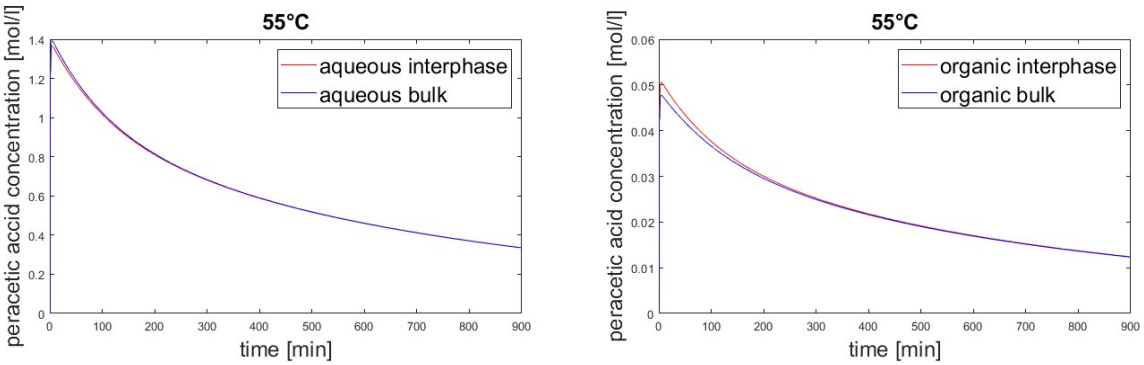

***Figure 4.9**. Time evolution of peracetic acid concentrations at the interphase and in the bulk of both organic and aqueous phase at 55°C.*

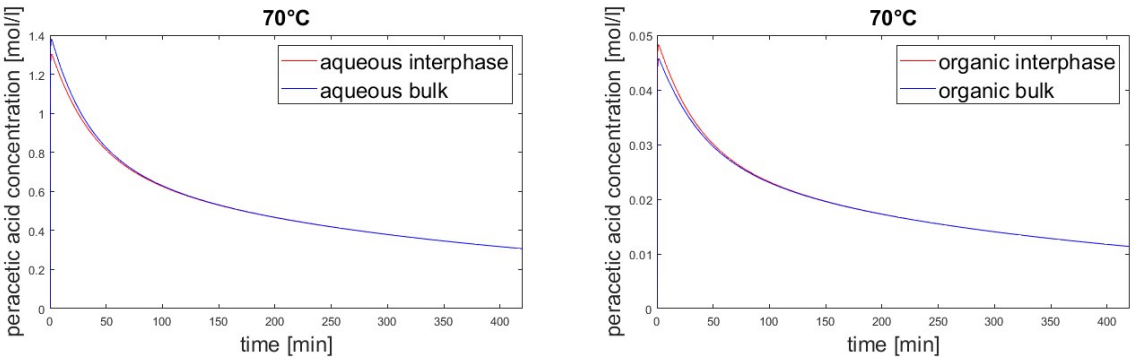

***Figure 4.10**. Time evolution of peracetic acid concentrations at the interphase and in the bulk of both organic and aqueous phase at 70°C.*

From the previous Figures it is noticed a greater difference between interphase and bulk peracetic acid concentration at 40°C, with respect to the two higher temperatures. Since both mass transfer and kinetic increase with temperature, this means that temperature has a bigger impact to mass transfer than kinetics. Even if in the case where the difference between bulk and

interphase concentrations is greater (40°C), their difference does not imply an initial mass transfer control but, at most a mixed regime. After 6 hours the profiles almost coincide suggesting a kinetic regime. In fact, if the concentrations at the interphase and in the bulk are very close, this means that the reaction cannot consume the reagent fast enough with respect to the rate at which it migrates from the aqueous phase to the organic one. At 55 and 70°C the concentration profiles are already almost coincident as soon as the reaction starts. For this reason, at the considered operating conditions, the process could always be under kinetic regime in the laboratory device.

Conclusions

In this work of thesis, a study on the epoxidation of soybean oil is carried out using peroxyacetic acid in a calorimetric reactor, performing a kinetic and a thermal study.

The main objective is the study of the epoxidation of soybean oil using peroxycarboxylic acid and hydrogen peroxide in presence of an acid liquid catalyst in order to develop a mathematical model able to simulate this specific epoxidation process. The model is developed with *MATLAB*® and information about the contribution of the reaction kinetics and the mass transfer between the two phases involved is obtained. This study is performed at three different operative temperatures: 40, 55 and 70°C at a constant stirring speed of 500 rpm.

Three data sets are experimentally obtained (one for each temperature) and from the experimental epoxide concentration values, it was possible the development of a bi-phasic mathematical model representative of the epoxidation process.

It describes the course of reaction well achieving a value of R^2 factor higher than 0.99 for each considered temperatures. From the kinetic constant values optimized by the model it was possible to calculate the pre-exponential factor and the activation energy related to the epoxidation reaction, which are equal to $7.16 \cdot 10^6$ $[kJ/mol]$ and 65.79 $[kJ/mol]$, respectively. The model also proves the kinetic regime of the epoxidation process under the chosen operating conditions in the laboratory scale. Further studies are due to establish the operating regime in larger reaction systems.

In addition, from a thermal study of the overall reaction system it was possible the determination of the global heat exchange coefficient equal to 2.215, 2.866 and 2.770 $[W/K]$ for 40, 55 and 70°C respectively. From this analysis, the mean global heat produced by the system is equal to -258$[kJ/mol]$, showing a great exothermicity.

The future improvements of this work could be the optimization by the model of the reaction orders of the kinetics considered as elementary. In addition, a modelling of the mass transfer coefficient taking into account droplet size and then also the stirring speed, would produce more accurate results throwing light on the local issues induced by the mass transfer. To finish, additional experimental data regarding other chemical species will allow the model parameters optimization not only with respect to the epoxides concentration.

Nomenclature

$\%OO$	=	oxirane oxygen content [%]
IV_0	=	initial iodine number of the oil [$g\ iodine/100g\ oil$]
A_I	=	atomic weight of iodine [g/mol]
A_0	=	atomic weight of oxygen [g/mol]
G	=	content of α-glycol [%]
A_{0H}	=	molecular weight of hydroxyl group [g/mol]
T_p	=	period of rotation [s]
n	=	number of divisions in the oscilloscope scale [-]
f	=	frequency [$ms/division$]
$\dot{Q}_{flow}$	=	heat flow [W]
$(U \cdot A)$	=	product between the heat transfer coefficient and the transfer area [W/K]
T	=	temperature [K]
T_j	=	jacket temperature [K]
$\dot{m}$	=	mass flow [kg/min]
cp	=	heat capacity [J/K]
t	=	time [min]
t_0	=	initial time [min]
N	=	number of moles [mol]
C	=	concentration [mol/l]
V	=	volume [ml]
Q	=	heat power [W]
P	=	heat power generated by the electric heater [W]
H	=	enthalpy [kJ/mol]
r	=	reaction rate [$mol/(l \cdot min)$]
k	=	kinetic constant (the unit depends on the reaction)
K	=	partition coefficient [-]
J	=	mass transfer rate [$mol/(l \cdot min)$]
$K_{1,eq}$	=	equilibrium constant of the peracetic acid production reaction [-]
A^{wo}	=	organic-aqueous interphase [m^2]
h_m	=	mass transfer coefficient [$1/(min \cdot m^2)$]
Err	=	mean squared error [-]
E_a	=	activation energy [kJ/mol]
A	=	pre-exponential factor [kJ/mol]
R	=	universal gas constant [$kJ/(mol \cdot K)$]

MW	=	molecular weight $[g/mol]$

Greek letters

ω	=	rotational speed [rpm]
$\hat{\rho}$	=	mass density $[g/l]$
υ	=	stochiometric coefficient [-]
τ	=	time constant [min]
β	=	product between the mass transfer coefficient and the interfacial area $[1/min]$

Acronyms

AA	=	acetic acid
PAA	=	peracetic acid
W	=	water
HP	=	hydrogen peroxide
EP	=	epoxides
$C = C$	=	unsaturated group (double bond)
EG	=	glycols

Subscripts and superscripts

o	=	organic phase
w	=	organic phase
i	=	interphase
b	=	bulk
j	=	generic species
the	=	theoretical
exp	=	experimental
in	=	inlet
out	=	outlet
ph	=	potassium phthalate
HBr	=	bromidic acid
d	=	dissipated
tot	=	total
→	=	direct
←	=	inverse

Bibliographic references

1. Quadros, J.V.Jr., R. Giudici (2015). Epoxidation of soybean oil at maximum heat Removal and single addition of all reactants. *Chemical Engineering and Processing*, **100**, 87-93.
2. E. Santacesaria, R. Tesser, M. Di Serio, R. Turco, V. Russo, D. Verde (2011). A biphasic model describing soybean oil epoxidation with H_2O_2 in a fed-batch reactor. *Chemical Engineering Journal*, **173**, 198 - 209.
3. Vaibhav V. Goud, Anand V. Patwardhan, Srikanta Dinda, Narayan C. Pradhan (2007). Kinetics of epoxidation of jatropha oil with peroxyacetic and peroxyformic acid catalysed by acidic ion exchange resin. *Chemical Engineering Science*, **62**, 4065 - 4076.
4. Kirk, R.E., Othmer, D.F., Mark, H.F., Standen, A., 1965. Kirk–Othmer. *Encyclopedia of Chemical Technology*. Wiley, New York.
5. Wanjie Li, Meifeng Tian, Haiyan Du, Zhenhai Liang (2015), A new approach for epoxidation of fatty acids by a paired electrosynthesis. *Electrochemistry Communications*, **54**, 46 - 50.
6. https://www.statista.com/statistics/263937/vegetable-oils-global-consumption/
7. Srikanta Dinda, Anand V. Patwardhan, Vaibhav V. Goud, Narayan C. Pradhan (2007). Epoxidation of cottonseed oil by acqueous hydrogen peroxide catalysed by liquid inorganic acids. *Bioresource Technology*, **99**, 3737 - 3744.
8. Chavan, V.P., A.V. Patwardhan, P.R. Gogate (2012). Intensification of epoxidation of soybean oil using sonochemical reactors. *Chemical Engineering and Processing*, **54**, 22 - 28.
9. Guenter, S., Rieth, R., Rowbottom, K.T. (2003). *6th ed. Ullmann's Encyclopedia of Industrial Chemistry*, vol. 12 John Wiley and Sons, 269 – 284.
10. Rios, L.A., Weckes, P., Schuster, H., Hoelderich, W.F. (2005). Mesoporous and amorphous Ti-silicas on the epoxidation of vegetables oils. J. Catal. **232**, 19 – 26.
11. Sharpeless, K.B., Woodard, S.S., Finn, M.G. (1983). On the mechanism of titanium tartrate catalyzed asymmetric epoxidation. *Pure Appl. Chem.*, 55, 1823 – 1836.
12. Sheldon, R.A., Dakka, J. (1994). Heterogeneous catalytic oxidations in the manufacture of fine chemicals. *Catal. Today*, **19**, 215 – 246.
13. E. Santacesaria, A. Renken, V. Russo, R. Turco, R. Tesser, M. Di Serio (2012). A biphasic model describing soybean oil epoxidation with H_2O_2 in continuous reactors. *Ind. Eng. Chem. Res.*, 51,8760-8767.
14. Leveneur, S., J. Zheng, B. Taouk, F. Burel, J. Warna. (2014). Interaction of thermal and kinetic parameters for a liquid-liquid reaction system: Application to vegetable oils

epoxidation by peroxycarboxylic acid. *Journal of the Taiwan Institute of Chemical Engineers,* **45**, 1449-1458.

15. Zhao, X., T. Zhang, Y. Zhou, D. Liu (2007). Preparation of peracetic acid from hydrogen peroxide Part I: Kinetics for peracetic acid synthesis and Hydrolysis. *Journal of Molecular Catalysis A: Chemical,* **271**, 246-252.
16. Zhao, X., K. Cheng, J. Hao, D. Liu (2008). Preparation of peracetic acid from hydrogen peroxide Part II: Kinetics for spontaneous decomposition of peracetic acid in the liquid phase. *Journal of Molecular Catalysis A: Chemical*, **284**, 58-68.
17. Leveneur, S., A. Ledoux, L. Estel, B. Taouk, T. Salmi (2014). Epoxidation of vegetable oils under microwave irradiation. *Chemical Engineering Research and Design*, **92**, 1495-1502.
18. Sinadinovic-Fiser, S., M. Jankovic, O. Borota (2012). Epoxidation of castor oil with peracetic acid formed *in situ* in the presence of a ion exchange resin. *Chemical Engineering and Processing*, **62**, 106-113.
19. Chavan, A., P. R. Gogate (2015). Ultrasound assisted synthesis of epoxidized sunflower oil and application as plasticizer. *Journal of Industrial and Engineering Chemistry*, **21**, 842-850.
20. Rangarajan, B., A. Havey, E. A. Grulke, D. Culnan (1995). Kinetic parameters of a two-phase model for in situ epoxidation of soybean oil. *Journal of the American Oil Chemists' Society*, **72**, 10.
21. Leveneur, S., A. Ledoux, L. Estel, B. Taouk, T. Salmi (2014). Epoxidation of vegetable oils under microwave irradiation. *Chemical Engineering Research and Design,* **92**, 1495-1502.
22. Sepulveda, J., S. Teixeira, U. Schuchardt (2006). Alumina-catalyzed epoxidation of unsaturated fatty esters with hydrogen peroxide. *Applied Catalysis A*, **318**, 213-217.
23. Jia, L. K., L. X. Gong, W. J. Ji, C. Y. Kan (2011). Synthesis of vegetable oil based polyol with cottonseed oil and sorbitol derived from natural sources. *Chinese Chemical Letters*, **22**, 1289-1292.
24. Juan C. de Haro, Irene Izarra, Juan F. Rodrìguez, Angel Perez, Manuel Carmona (2016). Modelling the epoxidation reaction of grape seed oil by peracetic acid. *Journal of Cleaner Production*, **138**,70-76.
25. American Oil Chemists' Society (2017). *Official methods and recommended practices of the AOCS*. Urbana. American Oil Chemists' Society.
26. E. Santacesaria, M. Di Serio, R. Tesser, V. Russo, R. Turco (2011). A new simple microchannel divide to test process intensification, *Ind. Eng. Chem. Res*., **50**, 2569-2575.
27. John La Scala and Richard P. Wool (2002). Effect of FA composition on epoxidation kinetics of TAG. J. Am. Oil Chem. Soc. **79** (2002) 373-378.

28. W. G. Whitman. Preliminary experimental confirmation of the two-film theory of gas absorption (1923). *Chem. Metall. Eng*. **29**, 146-148.
29. L.-K. Wu, K.-Y. Chen, S.-Y. Cheng, B.-S. Lee and C.-M. Shu (2008). Thermal decomposition of hydrogen peroxyde in the presence of sulfuric acid. *Journal of Thermal Analysis and Calorimetry*, **93**, 115-120.
30. V. Casson and G. Maschio (2011). Screening analysis for Hazar Assessment of peroxides decomposition. *Ind. Eng. Chem. Res.*, 7526-7535.
31. https://www.sigmaaldrich.com/catalog/product/supelco/47122?lang=it&region=IT
32. Damiano Piccolo, Chiara Vianello, Giuseppe Maschio (2017). A Complete Approach for the Determination of the Heat Exchange Coefficient of a Calorimetric Reactor. *Chemical Engineering transactions*, **57**, 1117-1122.
33. Saha, M. S., Y. Nishiki, T. Furuta, A. Denggerile, T. Ohsaka (2003). A new method for the preparation of peroxyacetic acid using solid superacid catalyst. *Tetrahedron Letters*, **44**, 5535-5537.
34. G. Sienel, R. Rieth, K. T. Rowbottom (2005), "Epoxides," *Ullmann's Encycl. Ind. Chem.*, 8676–8694.
35. W. J. Souza, K. M. C. Santos, A. A. Cruz, E. Francschi, C. Dariva, A. F. Santos, C. C. Santana (2014). Effect of water content, temperature and average droplet size on the settling velocity of water-in-oil emulsions. *Brazilian Journal of Chemical Engineering*, **32**, 445-464.